

# 331 Models Facing the Tensions in $\Delta F = 2$ Processes with the Impact on $\varepsilon'/\varepsilon$ , $B_s \rightarrow \mu^+\mu^-$ and $B \rightarrow K^*\mu^+\mu^-$

Andrzej J. Buras<sup>a,b</sup> and Fulvia De Fazio<sup>c</sup>

<sup>a</sup>TUM Institute for Advanced Study, Lichtenbergstr. 2a, D-85747 Garching, Germany

<sup>b</sup>Physik Department, Technische Universität München, James-Frank-Straße,  
D-85747 Garching, Germany

<sup>c</sup>Istituto Nazionale di Fisica Nucleare, Sezione di Bari, Via Orabona 4, I-70126 Bari, Italy

## Abstract

Motivated by the recently improved results from the Fermilab Lattice and MILC Collaborations on the hadronic matrix elements entering  $\Delta M_{s,d}$  in  $B_{s,d}^0 - \bar{B}_{s,d}^0$  mixings and the resulting increased tensions between  $\Delta M_{s,d}$  and  $\varepsilon_K$  in the Standard Model (SM) and CMFV models, we demonstrate that these tensions can be removed in 331 models based on the gauge group  $SU(3)_C \times SU(3)_L \times U(1)_X$  both for  $M_{Z'}$  in the LHC reach and well beyond it. But the implied new physics (NP) patterns in  $\Delta F = 1$  observables depend sensitively on the value of  $|V_{cb}|$ . Concentrating the analysis on three 331 models that have been selected by us previously on the basis of their performance in electroweak precision tests and  $\varepsilon'/\varepsilon$  we illustrate this for  $|V_{cb}| = 0.042$  and  $|V_{cb}| = 0.040$ . We find that these new lattice data still allow for positive shifts in  $\varepsilon'/\varepsilon$  up to  $6 \times 10^{-4}$  for  $M_{Z'} = 3$  TeV and  $|V_{ub}| = 0.0036$  for both values of  $|V_{cb}|$  but for  $M_{Z'} = 10$  TeV only for  $|V_{cb}| = 0.040$  such shifts can be obtained. For  $|V_{ub}| = 0.0042$  maximal shifts in  $\varepsilon'/\varepsilon$  increase to  $\simeq 7 \times 10^{-4}$ . NP effects in  $B_s \rightarrow \mu^+\mu^-$  and in the Wilson coefficient  $C_9$  are significantly larger in all three models for the case of  $|V_{cb}| = 0.040$ . In particular in two models the rate for  $B_s \rightarrow \mu^+\mu^-$  can be reduced by NP by 20% for  $M_{Z'} = 3$  TeV resulting in values in the ballpark of central values from CMS and LHCb. In the third model a shift in  $C_9$  up to  $C_9^{\text{NP}} = -0.5$  is possible. For  $|V_{cb}| = 0.042$ , NP effects in  $B_s \rightarrow \mu^+\mu^-$  and in  $C_9$  are by at least a factor of two smaller. For  $M_{Z'} = 10$  TeV NP effects in  $B_s \rightarrow \mu^+\mu^-$  and  $C_9$ , independently of  $|V_{cb}|$ , are at most at the level of a few percent. We also consider the simplest 331 model, analyzed recently in the literature, in which  $X = Y$ , the usual hypercharge. We find that in this model NP effects in flavour observables are much smaller than in the three models with  $X \neq Y$ , in particular NP contributions to the ratio  $\varepsilon'/\varepsilon$  are very strongly suppressed. Our analysis exhibits the important role of lattice QCD and of precise values of CKM parameters, in particular  $|V_{cb}|$ , for quark flavour phenomenology beyond the SM. It also demonstrates exceptional role of  $\Delta F = 2$  observables and of  $\varepsilon'/\varepsilon$  in testing high energy scales beyond the LHC.

# Contents

<b>1</b>	<b>Introduction</b>	<b>1</b>
<b>2</b>	<b>M8, M9 and M16 Facing Anomalies</b>	<b>4</b>
2.1	Preliminaries . . . . .	4
2.2	Numerical Analysis . . . . .	5
2.3	$ V_{cb} $ and $ V_{ub} $ Dependence . . . . .	10
2.4	$Z'$ Outside the Reach of the LHC . . . . .	13
2.4.1	$ V_{ub}  = 0.042$ . . . . .	13
2.4.2	$ V_{cb}  = 0.040$ . . . . .	15
<b>3</b>	<b>The Simplest 331 Model: M0</b>	<b>16</b>
3.1	Preliminaries . . . . .	16
3.2	$Z'$ Couplings . . . . .	16
3.3	$Z$ Couplings . . . . .	17
3.4	$C_9^{\text{NP}}$ and $C_{10}^{\text{NP}}$ . . . . .	17
3.5	$\varepsilon'/\varepsilon$ . . . . .	19
3.5.1	Preliminaries . . . . .	19
3.5.2	$Z$ Contribution . . . . .	19
<b>4</b>	<b>Summary</b>	<b>21</b>

## 1 Introduction

The Standard Model (SM) describes globally the existing data on quark-flavour violating processes rather well [1] but with the reduction of experimental errors and increased precision in non-perturbative and perturbative QCD and electroweak calculations a number of tensions at the level of  $2 - 3\sigma$  seem to emerge in various seemingly unrelated observables. While some of these tensions could turn out to be the result of statistical fluctuations, underestimate of systematical and theoretical errors, it is not excluded that eventually they all signal the presence of some kind of new physics (NP). Therefore, it is interesting to investigate what this NP could be.

In the present paper we will address some of these tensions in 331 models based on the gauge group  $SU(3)_C \times SU(3)_L \times U(1)_X$  [2,3]. As these models have much smaller number of new parameters than supersymmetric models, Randall-Sundrum scenarios and Littlest Higgs models, it is not evident that they can remove all present tensions simultaneously.

Our paper has been motivated by a recent analysis in [4] which demonstrates that the new lattice QCD results from Fermilab Lattice and MILC Collaborations [5] on  $B_{s,d}^0 - \bar{B}_{s,d}^0$  hadronic matrix elements imply a significant tension between  $\varepsilon_K$  and  $\Delta M_{s,d}$  within the SM. The authors of [5] find also inconsistencies between  $\Delta M_{s,d}$  and tree-level determination of  $|V_{cb}|$ . But the simultaneous consideration of  $\varepsilon_K$  and  $\Delta M_{s,d}$  in [4] also demonstrates that the tension between these two quantities cannot be removed for any value of  $|V_{cb}|$ . Moreover, the situation worsens for other models with constrained MFV (CMFV), indicating the presence of new flavour- and CP-violating interactions beyond CMFV framework at work.

The question then arises how 331 models face this tension and what are the implications of new lattice results on other observables for which some departures from SM predictions have been identified. In particular, taking the results in [4, 5] into account we want to concentrate our analysis on

$$\varepsilon'/\varepsilon, \quad B_s \rightarrow \mu^+\mu^-, \quad B \rightarrow K^*\mu^+\mu^-. \quad (1)$$

In this context the following facts should be recalled.

- Recent analyses in [6–9] find the ratio  $\varepsilon'/\varepsilon$  in the SM to be significantly below the experimental world average from NA48 [10] and KTeV [11, 12] collaborations. The recent analysis in the large  $N$  approach in [13] indicates that final state interactions will not modify this picture at least on the qualitative level. The analysis in [14] shows that CMFV models cannot cure this problem. In any case models providing an enhancement of  $\varepsilon'/\varepsilon$  should be favoured from present perspective.
- The branching ratio for  $B_s \rightarrow \mu^+\mu^-$  measured by CMS and LHCb [15] has been always visibly below rather precise prediction of the SM [16]. The most recent result from ATLAS<sup>1</sup>, while not accurate, appears to confirm this picture and models suppressing the rate for this decay relative to its SM prediction appear to be favoured.
- LHCb data on  $B_d \rightarrow K(K^*)\mu^+\mu^-$  indicate some departures from SM expectation although this issue is controversial. See [18, 19] and references to the rich literature therein. Assuming again that statistical fluctuations or underestimated errors are not responsible for these effects, significant NP contributions to the Wilson coefficient  $C_9$  or  $C_9$  and  $C_{10}$  are required.

These three items have been already addressed by us within 331 models in the past [20–23]. In particular in [23] the issue of  $\varepsilon'/\varepsilon$  anomaly has been addressed, while in [21, 23] the last two items above have been considered. The main result of [23] is that among 24 331 models only three (M8, M9 and M16 in the terminology of [22]) have a chance to survive if an improved fit to electroweak precision observables relative to the SM is required and the  $\varepsilon'/\varepsilon$  anomaly will be confirmed in the future. Two of them (M8 and M9) allowed simultaneously a suppression of the rate for  $B_s \rightarrow \mu^+\mu^-$  by 20% thereby bringing the theory closer to the data without any significant impact on the Wilson coefficient  $C_9$ . The third model (M16) provided, simultaneously to the enhancement of  $\varepsilon'/\varepsilon$ , a shift up to  $\Delta C_9 = -0.6$ , softening the anomalies in  $B \rightarrow K^*\mu^+\mu^-$ , without any significant impact on  $B_s \rightarrow \mu^+\mu^-$ . While, before the ATLAS data on  $B_s \rightarrow \mu^+\mu^-$ , M16 seemed to be slightly favoured over M8 and M9, this data and the fact that the theoretical uncertainties in  $B_s \rightarrow \mu^+\mu^-$  are significantly smaller than in  $B_d \rightarrow K^*\mu^+\mu^-$  make us believe that at the end models M8 and M9 have a bigger chance to survive.

However, the constraints from  $\Delta F = 2$  transitions used in [23], prior to the lattice QCD result in [5], were significantly weaker and it is of interest to investigate what is the impact of these new lattice results on our previous analyses and whether the increased tension between  $\varepsilon_K$  and  $\Delta M_{s,d}$  within the SM pointed out in [4] can be removed in these three models. In fact one should recall that the mixing and CP-violation in  $B_{s,d}^0 - \bar{B}_{s,d}^0$  systems play very important

---

<sup>1</sup> $\overline{B}(B_s \rightarrow \mu^+\mu^-) = (0.9_{-0.9}^{+1.1}) \times 10^{-9}$  [17].

roles in the determination of new parameters in 331 models [20] and it is not surprising that our previous results will be indeed modified in a visible manner.

In this context let us remark that within the SM, dependently on whether  $\Delta M_s$  or  $\varepsilon_K$  has been used as a constraint, rather different values for  $|V_{cb}|$  have been required to fit the data within the SM [4]:

$$|V_{cb}| = (39.7 \pm 1.3) \times 10^{-3} \quad (\Delta M_s), \quad |V_{cb}| = (43.3 \pm 1.1) \times 10^{-3} \quad (\varepsilon_K). \quad (2)$$

This in turn resulted in rather different predictions for rare  $K$  and  $B_{s,d}$  decays as seen in Table 4 of [4].

In our most recent analysis in [23] we have performed numerical analysis for  $|V_{cb}|$  in the ballpark of the higher value in (2), that is 0.042. In the present paper we will also use this value in order to see the impact of new lattice data on our previous results, but in addition we will perform the analysis with 0.040 which is in the ballpark of its lower value in (2). This will tell us whether 331 models can cope with the tensions in question for both values of  $|V_{cb}|$  and whether the implications for NP effects are modified through this change of  $|V_{cb}|$ .

The second motivation for a new analysis of 331 models is the following one. In our analyses and also in [24–26] the  $U(1)_X$  factor in the gauge group  $SU(3)_C \times SU(3)_L \times U(1)_X$  differed from the hypercharge gauge group  $U(1)_Y$ . As various 331 models are characterized by two parameters  $\beta$  and  $\tan \bar{\beta}$  defined through

$$Q = T_3 + \frac{Y}{2} = T_3 + \beta T_8 + X, \quad \tan \bar{\beta} = \frac{v_\rho}{v_\eta} \quad (3)$$

these analyses dealt with  $\beta \neq 0$ . Here  $T_{3,8}$  and  $X$  are the diagonal generators of  $SU(3)_L$  and  $U(1)_X$ , respectively.  $Y$  represents  $U(1)_Y$  and  $v_i$  are the vacuum expectation values of scalar triplets responsible for the generation of down- and up-quark masses in these models.

Recently a special variant of 331 models with  $\beta = 0$  or equivalently  $U(1)_X = U(1)_Y$  has been considered in [27]. Moreover, these authors set  $\tan \bar{\beta} = 1$  as this choice with  $\beta = 0$  simplifies the model by eliminating  $Z - Z'$  mixing studied by us in detail in [22] for  $\beta \neq 0$ . As this is the simplest among the 331 models, the question arises whether it is consistent with the flavour data in the setup in [27] and what are the implications for quark flavour observables for arbitrary  $\tan \bar{\beta}$  when  $Z - Z'$  mixing enters the game. In particular the comparison with our studies for  $\beta \neq 0$  in [20–23] and in the present paper is of interest. As the authors of [27] did not address this question, to our knowledge this is the first quark flavour study of this simplified 331 model.

We will see that in the absence of  $Z - Z'$  mixing the choice  $\beta = 0$  provides a unique 331 model in which the phenomenologically successful relation

$$C_9^{\text{NP}} = -C_{10}^{\text{NP}} \quad (4)$$

is satisfied. Here  $C_9^{\text{NP}}$  and  $C_{10}^{\text{NP}}$  stand for the shifts in the Wilson coefficients relevant in particular for  $B \rightarrow K^* \mu^+ \mu^-$  and  $B_s \rightarrow \mu^+ \mu^-$ , respectively. This is good news. The bad news is that setting  $\beta = 0$  modifies the values of all couplings relative to the ones in M8, M9 and M16 models. We find then that NP contributions to  $\varepsilon'/\varepsilon$  in this simple model are at most  $1 \times 10^{-4}$  for  $M_{Z'} = 3 \text{ TeV}$  and decrease with increasing  $M_{Z'}$ . The effects in  $C_9^{\text{NP}}$  and  $C_{10}^{\text{NP}}$  are at most at the level of a few percent even if  $Z - Z'$  mixing is taken into account. Thus the

model fails in solving three anomalies listed above. But as we will see it is able to remove the tensions between  $\Delta M_{s,d}$  and  $\varepsilon_K$ .

Our paper is organized as follows. In Section 2 we address the tensions between  $\Delta M_{s,d}$  and  $\varepsilon_K$  in M8, M9 and M16 models and we update our analysis of  $\varepsilon'/\varepsilon$ ,  $B_s \rightarrow \mu^+ \mu^-$  and  $C_9$  in [23] taking new  $\Delta F = 2$  constraints from [5] into account and performing the analysis at two values of  $|V_{cb}|$  as discussed above. In Section 3 we specify the existing formulae in 331 models to the case  $\beta = 0$  but for arbitrary  $\tan \bar{\beta}$  and we derive the results mentioned above. We conclude in Section 4.

## 2 M8, M9 and M16 Facing Anomalies

### 2.1 Preliminaries

Let us recall that in these three models new flavour-violating effects are governed by tree-level  $Z'$  exchanges with a subdominant role played by tree-level  $Z$  exchanges generated through  $Z - Z'$  mixing. All the formulae for flavour observables in these models can be found in [20–23] and will not be repeated here. In particular the collection of formulae for  $Z'$  couplings to quarks and leptons for arbitrary  $\beta$  are given in (17) and (18) of [21].

New sources of flavour and CP violation in 331 models are parametrized by new mixing parameters and phases

$$\tilde{s}_{13}, \quad \tilde{s}_{23}, \quad \delta_1, \quad \delta_2 \quad (5)$$

with  $\tilde{s}_{13}$  and  $\tilde{s}_{23}$  positive definite and smaller than unity and  $0 \leq \delta_{1,2} \leq 2\pi$ . They can be constrained by flavour observables as demonstrated in detail in [20]. The non-diagonal  $Z'$  couplings relevant for  $K$ ,  $B_d$  and  $B_s$  meson systems can be then parametrized respectively within an excellent approximation through

$$v_{32}^* v_{31} = \tilde{s}_{13} \tilde{s}_{23} e^{i(\delta_2 - \delta_1)}, \quad v_{33}^* v_{31} = -\tilde{s}_{13} e^{-i\delta_1}, \quad v_{33}^* v_{32} = -\tilde{s}_{23} e^{-i\delta_2}. \quad (6)$$

$\tilde{s}_{13}$  and  $\delta_1$  can be determined from  $\Delta M_d$  and CP-asymmetry  $S_{\psi K_S}$  while  $\tilde{s}_{23}$  and  $\delta_2$  from  $\Delta M_s$  and CP-asymmetry  $S_{\psi\phi}$ . Then the parameters in the  $K$  system are fixed. This correlation tells us that the removal of tensions between  $\varepsilon_K$  and  $\Delta M_{s,d}$  is not necessarily automatic in 331 models and constitutes an important test of these models.

The remaining two parameters, except for  $M_{Z'}$  mass, are as seen in (3),  $\beta$  and  $\tan \bar{\beta}$ . Moreover, the fermion representations of SM quarks under the  $SU(3)_L$  group matter. The three models in question are then characterized by

$$\beta = \frac{2}{\sqrt{3}}, \quad \tan \bar{\beta} = 5 \quad (F_1), \quad (\text{M8}), \quad (7)$$

$$\beta = -\frac{2}{\sqrt{3}}, \quad \tan \bar{\beta} = 1 \quad (F_2), \quad (\text{M9}), \quad (8)$$

$$\beta = \frac{2}{\sqrt{3}}, \quad \tan \bar{\beta} = 5 \quad (F_2), \quad (\text{M16}) \quad (9)$$

with  $F_1$  and  $F_2$  standing for two fermion representations. In  $F_1$  the first two generations of quarks belong to triplets of  $SU(3)_L$ , while the third generation of quarks to an antitriplet. In

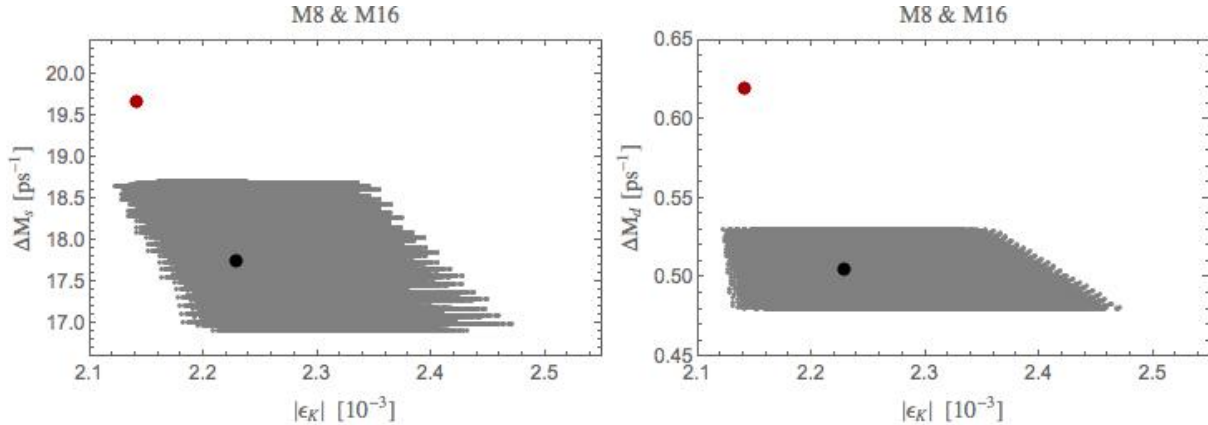


Figure 1:  $\Delta M_{s,d}$  vs.  $\varepsilon_K$  in M8 and M16. Red dots represent central SM values, black dots the central experimental values.  $M_{Z'} = 3 \text{ TeV}$  and  $|V_{cb}| = 0.042$ .

$F_2$  it is opposite. With the values of  $\beta$  and  $\tan \bar{\beta}$  being fixed flavour phenomenology depends only on the parameters in (5) and  $M_{Z'}$ .

## 2.2 Numerical Analysis

The difficulty in doing the numerical analysis are tensions between inclusive and exclusive determinations of the CKM elements  $|V_{cb}|$  and  $|V_{ub}|$ . The exclusive determinations have been summarized in [28] and are given as follows

$$|V_{cb}|_{\text{excl}} = (39.78 \pm 0.42) \cdot 10^{-3}, \quad |V_{ub}|_{\text{excl}} = (3.59 \pm 0.09) \cdot 10^{-3}. \quad (10)$$

They are based on [5, 29–32]. The inclusive ones are summarized well in [33, 34]

$$|V_{cb}|_{\text{incl}} = (42.21 \pm 0.78) \cdot 10^{-3}, \quad |V_{ub}|_{\text{incl}} = (4.40 \pm 0.25) \cdot 10^{-3}. \quad (11)$$

We note that after the recent Belle data on  $B \rightarrow D\ell\nu_l$  [31], the exclusive and inclusive values of  $|V_{cb}|$  are closer to each other than in the past. On the other hand in the case of  $|V_{ub}|$  there is a very significant difference.

Furthermore, after recent precise determinations of hadronic matrix elements entering  $\Delta M_{s,d}$  in  $B_{s,d}^0 - \bar{B}_{s,d}^0$  mixing by Fermilab Lattice and MILC Collaborations [5] there are significant tensions between tree-level determinations of  $|V_{cb}|$  and  $|V_{ub}|$  and  $\Delta M_{s,d}$  within the SM [5] and also the tensions between  $\varepsilon_K$  and  $\Delta M_{s,d}$  [4] in this model. Moreover, as found in the latter paper, the value of the angle  $\gamma$  in the unitarity triangle extracted from the ratio  $\Delta M_d/\Delta M_s$  and the CP-asymmetry  $S_{\psi K_S}$  is with  $\gamma = (63.0 \pm 2.1)^\circ$  visibly smaller than it tree-level determination [35]

$$\gamma = (73.2_{-7.0}^{+6.3})^\circ. \quad (12)$$

In the present paper, as in [23], we will set first the CKM parameters to

$$|V_{ub}| = 3.6 \times 10^{-3}, \quad |V_{cb}| = 42.0 \times 10^{-3}, \quad \gamma = 70^\circ. \quad (13)$$

This choice is in the ballpark of exclusive determination of  $|V_{ub}|$  in (10) and the inclusive one for  $|V_{cb}|$  in (11). Moreover, it is in the ballpark of tree-level determination of  $\gamma$ . In view of

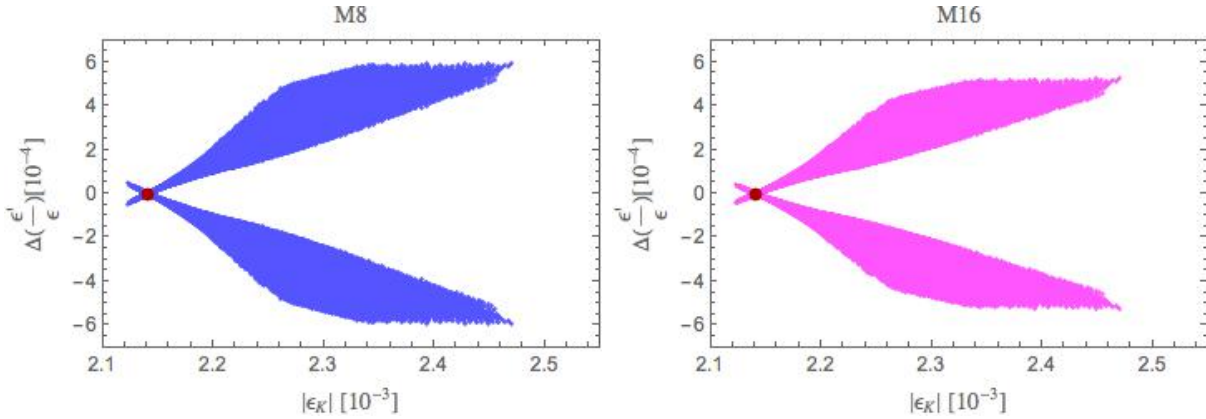


Figure 2:  $\Delta(\varepsilon'/\varepsilon)$  versus  $\varepsilon_K$  for *M8* and *M16*. Red dots represent central SM values.  $M_{Z'}$  = 3 TeV and  $|V_{cb}| = 0.042$ .

new parameters in 331 models the value of  $\gamma$  does not follow from the ratio  $\Delta M_s/\Delta M_d$  and  $S_{\psi K_S}$  like in CMFV models and it is better to take  $\gamma$  from tree-level determinations as it is to first approximation not polluted by NP. Having the same CKM input as in our previous analysis will allow us to see the impact of new lattice data on phenomenology.

The choice in (13) is also motivated by the fact that NP contributions to  $\varepsilon_K$  in 331 models are rather small for  $M_{Z'}$  of a few TeV and SM should perform well in this case. Indeed for this choice of CKM parameters we find

$$|\varepsilon_K|_{\text{SM}} = 2.14 \times 10^{-3}, \quad (\Delta M_K)_{\text{SM}} = 0.467 \cdot 10^{-2} \text{ ps}^{-1} \quad (14)$$

and  $|\varepsilon_K|$  in the SM only 4% below the data. Due to the presence of long distance effects in  $\Delta M_K$  also this value is compatible with the data.

While the CKM parameters do not enter the shift in  $\varepsilon'/\varepsilon$  and  $\varepsilon_K$ , their choice matters in the predictions for NP contributions to  $\Delta F = 2$  observables in  $B_{d,s}^0 - \bar{B}_{d,s}^0$  systems and the rare  $B_{s,d}$  decays. This is not only because of their interferences with SM contributions. The departure of SM predictions for  $\varepsilon_K$  and  $\Delta M_{s,d}$  from the data depends on the CKM parameters, in particular on the value of  $|V_{cb}|$ , and this has an impact on the allowed ranges of new parameters extracted from  $\Delta F = 2$  observables and consequently on final values of  $\varepsilon'/\varepsilon$ ,  $\bar{\mathcal{B}}(B_s \rightarrow \mu^+ \mu^-)$  and the shift in  $C_9$ . We will illustrate this below by choosing also  $|V_{cb}| = 0.040$  which corresponds to its exclusive determination in (10). See (23).

Next, as in [20, 23], we perform a simplified analysis of  $\Delta M_{d,s}$ ,  $S_{\psi K_S}$  and  $S_{\psi\phi}$  in order to identify oases in the space of four parameters (5) for which these four observables are consistent with experiment. To this end we use the formulae for  $\Delta F = 2$  observables in [20, 22] and set input parameters listed in Table 3 of our recent analysis in [23] at their central values. The only modifications in this input are the recently calculated parameters [5]<sup>2</sup>

$$F_{B_s} \sqrt{\hat{B}_{B_s}} = (274.6 \pm 8.8) \text{ MeV}, \quad F_{B_d} \sqrt{\hat{B}_{B_d}} = (227.7 \pm 9.8) \text{ MeV}, \quad (15)$$

<sup>2</sup>These results are more accurate than ETM results [36], but compatible with them. We look forward to new FLAG averages on these quantities.

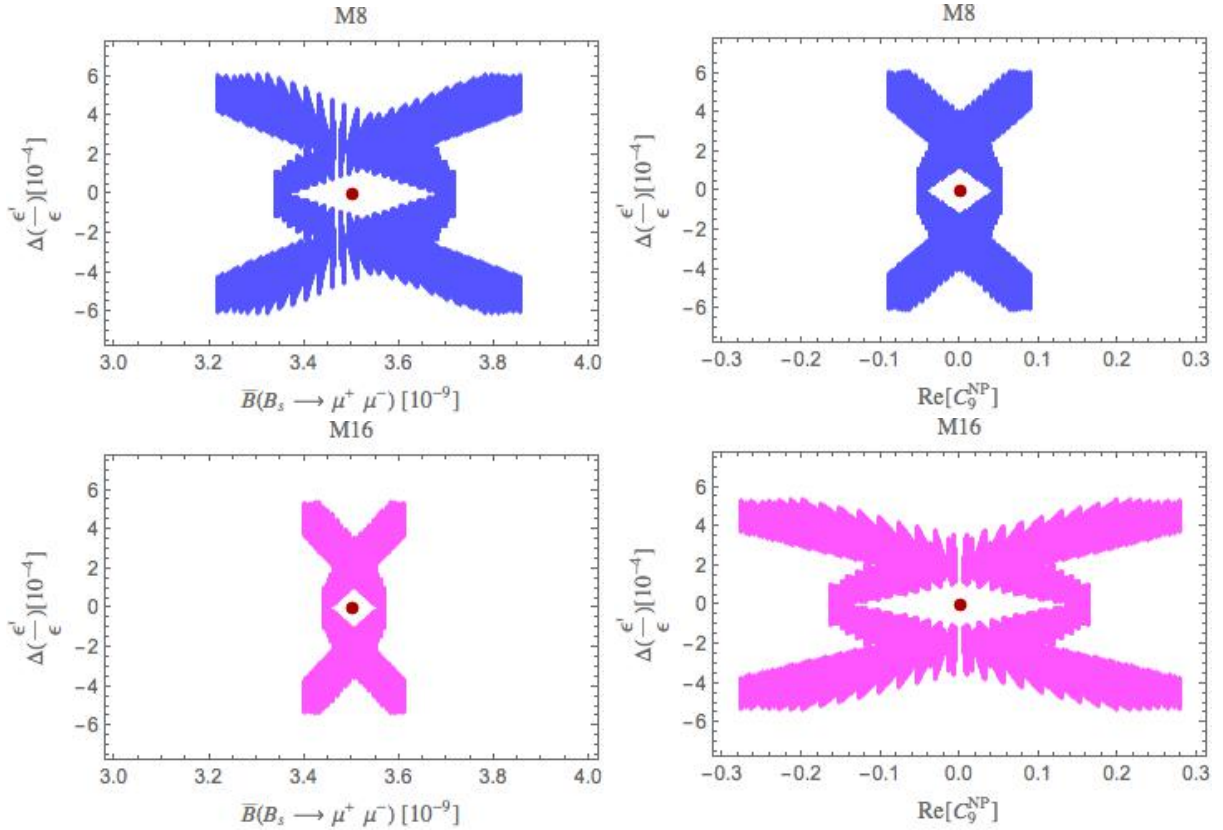


Figure 3: Correlations of  $\Delta(\varepsilon'/\varepsilon)$  with  $B_s \rightarrow \mu^+\mu^-$  (left panels) and with  $C_9^{\text{NP}}$  (right panels) for M8 and M16. Red dots represent central SM values.  $M_{Z'} = 3 \text{ TeV}$  and  $|V_{cb}| = 0.042$ .

that should be compared with  $F_{B_s}\sqrt{\hat{B}_{B_s}} = (266.0 \pm 18.0) \text{ MeV}$  and  $F_{B_d}\sqrt{\hat{B}_{B_d}} = (216.0 \pm 15.0) \text{ MeV}$  used by us in [23]. This change implies the modifications in the SM values of  $\Delta M_{s,d}$  that now are significantly higher than the data:

$$(\Delta M_s)_{\text{SM}} = 19.66/\text{ps}, \quad (\Delta M_d)_{\text{SM}} = 0.620/\text{ps}, \quad S_{\psi\phi}^{\text{SM}} = 0.037, \quad S_{\psi K_S}^{\text{SM}} = 0.688 \quad (16)$$

with CP asymmetries unchanged and compatible with the data. Thus the 331 models are requested to bring the values of  $\Delta M_{s,d}$  down to their experimental values [37]

$$(\Delta M_s)_{\text{exp}} = 17.757(21)/\text{ps}, \quad (\Delta M_d)_{\text{exp}} = 0.5055(20)/\text{ps}, \quad (17)$$

while being consistent with the data for  $\varepsilon_K$ ,  $S_{\psi K_S}$  and  $S_{\psi\phi}$ .

As we keep the input parameters at their central values, in order to take partially hadronic and experimental uncertainties into account we require the 331 models to reproduce the data for  $\Delta M_{s,d}$  within  $\pm 5\%$  and the data on  $S_{\psi K_S}$  and  $S_{\psi\phi}$  within experimental  $2\sigma$  ranges.

Specifically, our search is governed by the following allowed ranges:

$$16.9/\text{ps} \leq \Delta M_s \leq 18.7/\text{ps}, \quad -0.055 \leq S_{\psi\phi} \leq 0.085, \quad (18)$$

$$0.48/\text{ps} \leq \Delta M_d \leq 0.53/\text{ps}, \quad 0.657 \leq S_{\psi K_S} \leq 0.725. \quad (19)$$



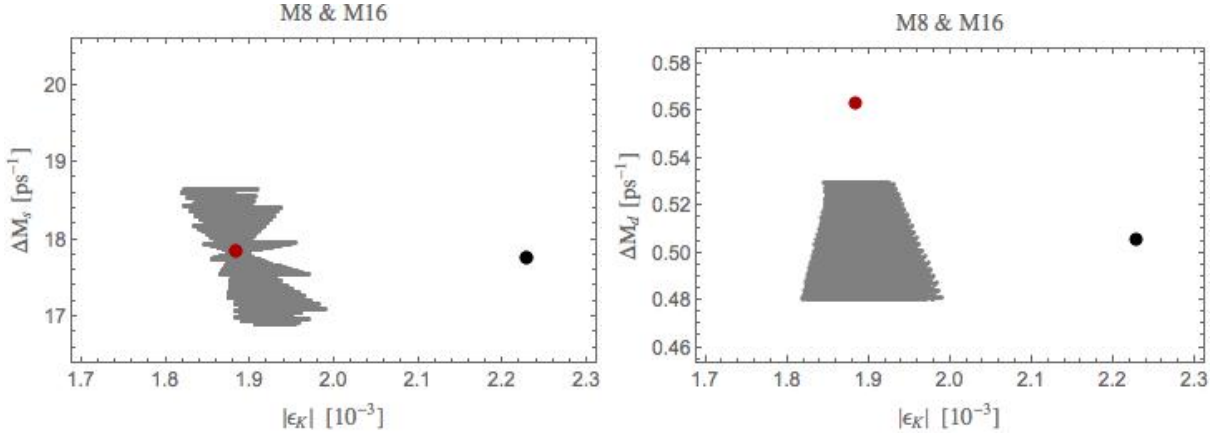


Figure 4:  $\Delta M_{s,d}$  vs.  $\varepsilon_K$  in M8 and M16. Red dots represent central SM values, black dots the central experimental values.  $M_{Z'} = 3 \text{ TeV}$ ,  $|V_{cb}| = 0.040$  and  $|V_{ub}| = 0.0036$ .

The ranges for  $\Delta M_{s,d}$  are smaller than used in [23] because of the reduced errors in (15).

We also impose the constraint on the ratio  $\Delta M_s/\Delta M_d$  using [5]

$$\xi = \frac{F_{B_s} \sqrt{\hat{B}_{B_s}}}{F_{B_d} \sqrt{\hat{B}_{B_d}}} = 1.206 \pm 0.019. \quad (20)$$

In the spirit of our simplified analysis we will keep this ratio at its central value in (20) but in order to take into account the uncertainty in  $\xi$  we will require that  $\Delta M_s/\Delta M_d$  agrees with the data within  $\pm 5\%$ . Specifically we will require that

$$33.3 \leq \left( \frac{\Delta M_s}{\Delta M_d} \right) \leq 36.8 \quad (21)$$

is satisfied.

In the case of  $\varepsilon_K$  and  $\Delta M_K$  we will just proceed as in [23] imposing the ranges

$$1.60 \times 10^{-3} < |\varepsilon_K| < 2.50 \times 10^{-3}, \quad -0.30 \leq \frac{(\Delta M_K)^{Z'}}{(\Delta M_K)_{\text{exp}}} \leq 0.30. \quad (22)$$

Having determined the ranges for the parameters (5) we can calculate all the remaining flavour observables of interest.

In Fig. 1 we show  $\Delta M_{s,d}$  vs.  $\varepsilon_K$  in M8 and M16. Red dots represent central SM values and black dots the central experimental values. The experimental errors are negligible and the parametric and theoretical errors are represented by the allowed departure from them as explained above. These results do not depend on the fermion representation up to tiny effects from  $Z - Z'$  mixing and consequently are practically the same for M8 and M16. As far as M9 is concerned all results presented in our paper are very similar to the ones in M8 and will not be shown. We observe that the tensions between  $\Delta M_{s,d}$  vs.  $\varepsilon_K$  present in the SM can be easily removed in 331 models for  $M_{Z'} = 3 \text{ TeV}$ .

In Fig. 2 we show  $\Delta(\varepsilon'/\varepsilon)$  versus  $\varepsilon_K$  for M8 and M16 at  $M_{Z'} = 3 \text{ TeV}$ . Taking the uncertainties due to charm contribution and CKM parameters in  $\varepsilon_K$  into account the maximal

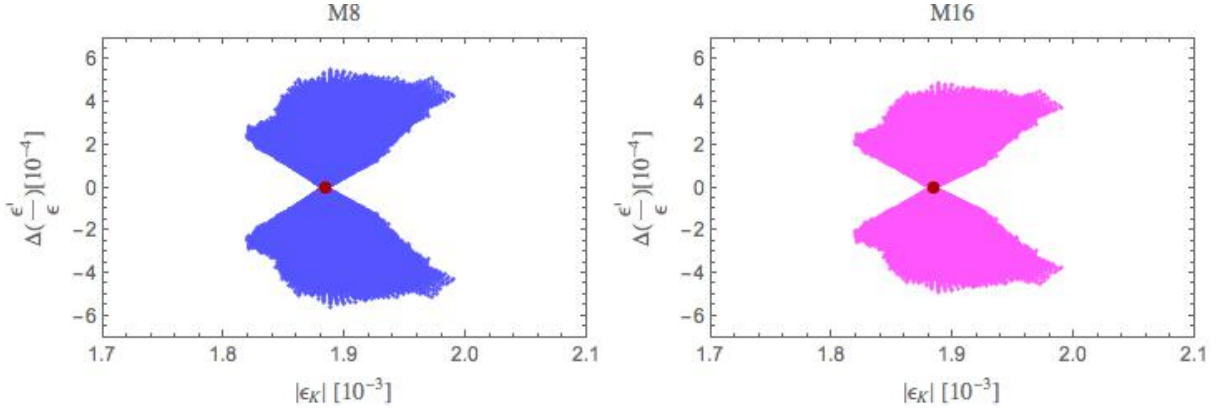


Figure 5:  $\Delta(\varepsilon'/\varepsilon)$  versus  $\varepsilon_K$  for M8 and M16. Red dots represent central SM values.  $M_{Z'}$  = 3 TeV,  $|V_{cb}| = 0.040$  and  $|V_{ub}| = 0.0036$ .

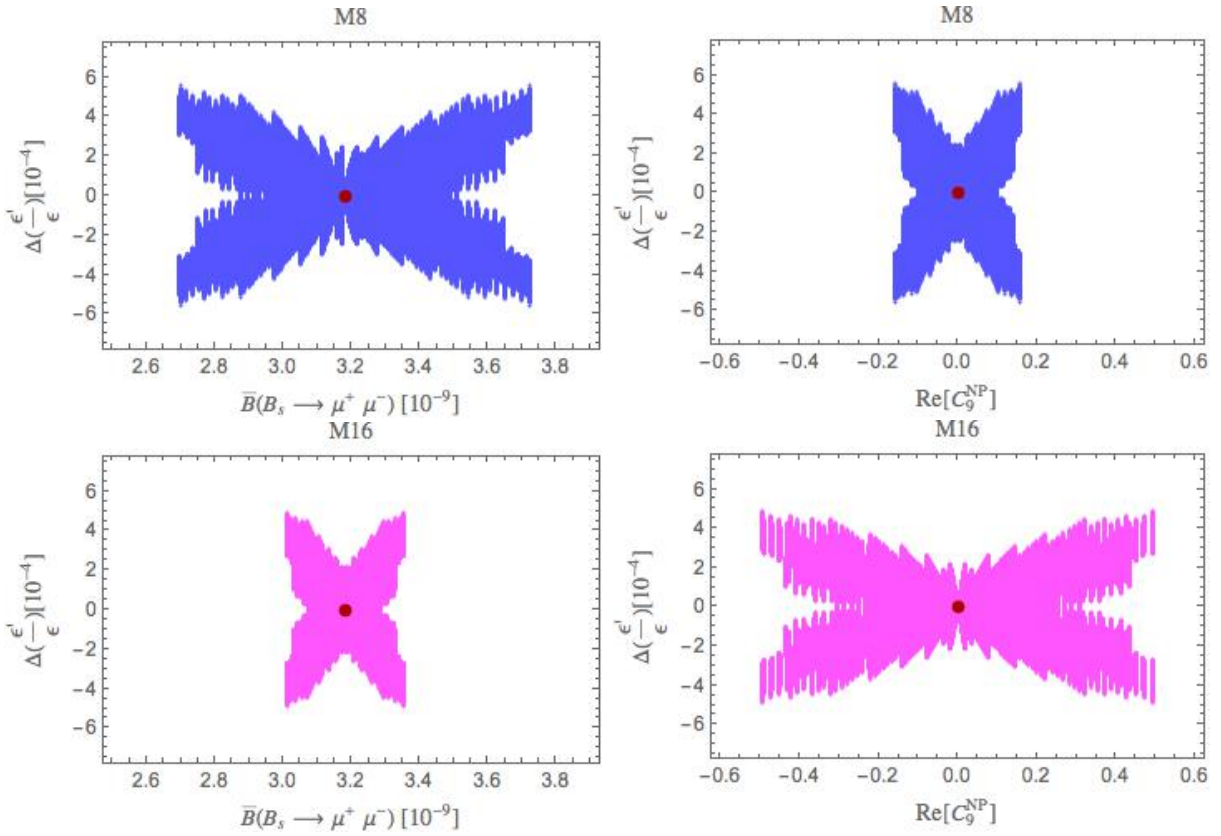


Figure 6: Correlations of  $\Delta(\varepsilon'/\varepsilon)$  with  $B_s \rightarrow \mu^+ \mu^-$  (left panels) and with  $C_9^{\text{NP}}$  (right panels) for M8 and M16. Red dots represent central SM values.  $M_{Z'}$  = 3 TeV,  $|V_{cb}| = 0.040$  and  $|V_{ub}| = 0.0036$ .

shifts in  $\varepsilon'/\varepsilon$  in both models amount to  $6 \times 10^{-4}$ , very similar to what we found in [23]. But NP effects in  $B_s \rightarrow \mu^+ \mu^-$  and  $C_9$  are smaller relative to the ones found in the latter paper by a factor of two. This is seen in Fig. 3, where we show correlations of  $\Delta(\varepsilon'/\varepsilon)$  with  $B_s \rightarrow \mu^+ \mu^-$

(left panels) and with  $C_9^{\text{NP}}$  (right panels) for M8 and M16 and  $M_{Z'} = 3 \text{ TeV}$ .

In M8 the rate for  $B_s \rightarrow \mu^+ \mu^-$  can be suppressed by 10% bringing the theory closer to the data in (24) [15]. Moreover, this happens for the largest shift in  $\varepsilon'/\varepsilon$ . But the shift in  $C_9$  is very small. In M16 the pattern is opposite with only a very small NP effects in  $B_s \rightarrow \mu^+ \mu^-$  and a shift of  $-0.3$  in  $C_9$  which brings the theory closer to the data.

### 2.3 $|V_{cb}|$ and $|V_{ub}|$ Dependence

It is well known that  $\varepsilon_K$  and  $\Delta M_{s,d}$  in the SM are sensitive functions of  $|V_{cb}|$ . Moreover,  $\varepsilon_K$  and  $S_{\psi K_S}$  depend sensitively on  $|V_{ub}|$ . Setting  $|V_{cb}|$  and  $|V_{ub}|$  to the values in (13) we have necessarily constrained the allowed range of NP parameters that are consistent with the data on  $\Delta F = 2$  observables. Changing  $|V_{cb}|$  and  $|V_{ub}|$  will necessarily modify this range and will modify NP contributions to flavour observables even if they do not depend directly on  $|V_{cb}|$  and  $|V_{ub}|$ . A sophisticated analysis which would include the uncertainties in both CKM elements from tree-level decays would wash out NP effects and would not teach us much about the impact of  $|V_{cb}|$  and  $|V_{ub}|$  on our results.

Therefore, we prefer to show how our results presented above are modified for a different value of  $|V_{cb}|$  that we choose to be lower so that instead of (13) we now use

$$|V_{ub}| = 3.6 \times 10^{-3}, \quad |V_{cb}| = 40.0 \times 10^{-3}, \quad \gamma = 70^\circ. \quad (23)$$

We keep  $|V_{ub}|$  and  $\gamma$  unchanged as this will allow us to see the role of  $|V_{cb}|$  better. The dependence on  $\gamma$  in the observables in question is weak. The dependence of  $\Delta M_{s,d}$  on  $|V_{ub}|$  is totally negligible. The inclusive value of  $|V_{ub}|$  would compensate the decrease of  $|V_{cb}|$  in  $\varepsilon_K$  but would simultaneously have an impact on  $S_{\psi K_S}$  shifting it in the ballpark of 0.80 within the SM. While in the SM this problem cannot be cured because of the absence of new CP-violating phases, in 331 models the presence of the phase  $\delta_1$  in (6) allows to satisfy the constraint on  $S_{\psi K_S}$  in (19). We will demonstrate it below.

This assures us that the tension between  $\varepsilon_K$  and  $S_{\psi K_S}$  for exclusive value of  $|V_{cb}|$  present in the SM can be avoided within the 331 models. But as we would like to investigate the impact of the change in  $|V_{cb}|$  on our results, we keep first  $|V_{ub}|$  at its exclusive value. Moreover there is some kind of consensus in the community that in the case of  $|V_{ub}|$  one can trust more exclusive determinations of this parameter than the inclusive ones. This is based on the fact that the exclusive determinations use formfactors from lattice QCD, which on the one hand are already rather precise and on the other hand do not require the assumptions like hadron duality necessary for the inclusive determination of  $|V_{ub}|$ .

The results of this exercise are shown in Figs. 4-6. Comparing Fig. 4 with Fig. 1 it is evident that 331 models perform better for our nominal choice of CKM parameters in (13) than for a lower value of  $|V_{cb}|$ . This is seen in particular in the case of  $\varepsilon_K$  for which the maximal values of  $\varepsilon_K$  are by 10% below the data. But, as discussed above, increasing  $|V_{ub}|$  towards its inclusive value and taking the uncertainties in the QCD corrections to the charm contribution in  $\varepsilon_K$  into account one can bring the theory much closer to data without violating the constraint on  $S_{\psi K_S}$  in (19). We demonstrate this in Fig. 7 where we use  $|V_{ub}| = 0.0042$ . Indeed  $\varepsilon_K$  is now in a perfect agreement with the data. The slight increase of the maximal value of  $\Delta(\varepsilon'/\varepsilon)$  in this case will be analyzed in more details below.

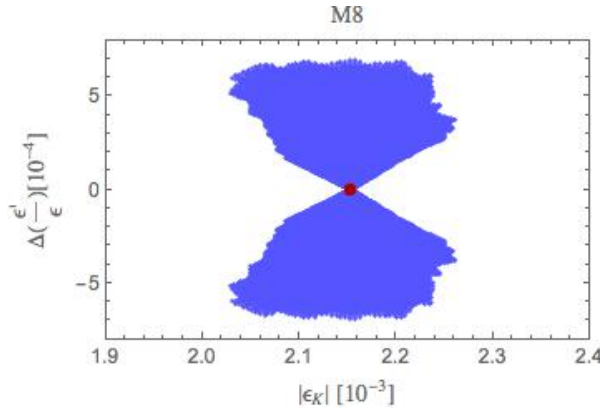


Figure 7:  $\Delta(\varepsilon'/\varepsilon)$  versus  $\varepsilon_K$  for M8. Red dot represents central SM value.  $M_{Z'}$  = 3 TeV,  $|V_{cb}| = 0.040$  and  $|V_{ub}| = 0.0042$ .

Therefore we can claim that 331 models also in this case remove the tensions in question, which is not possible within the SM. Interestingly, as we will see below for significantly higher values of  $M_{Z'}$  the removal of tensions for this value of  $|V_{cb}|$  will be much easier. We refer to Section 4 in [23] for the explanation of this behaviour.

Next Figs. 5 and 6 should be compared with Figs. 2 and 3, respectively. We observe:

- The correlation between  $\varepsilon'/\varepsilon$  and  $\varepsilon_K$  in Fig. 5 has a very different shape than in Fig. 2 but a shift of  $\varepsilon'/\varepsilon$  of  $(5 - 6) \times 10^{-4}$  is possible. In fact this plot is similar to a corresponding plot in [23] obtained with CKM parameters in (13) but older hadronic matrix elements. This similarity is easy to understand. The increase of non-perturbative parameters in (15) has been roughly compensated by the decrease of  $|V_{cb}|$ .
- The size of NP effects in  $B_s \rightarrow \mu^+\mu^-$  and  $C_9$  is now larger than for our nominal value of  $|V_{cb}|$  and similar to the ones found in [23]: suppression of the rate for  $B_s \rightarrow \mu^+\mu^-$  by 20% in the case of M8 and a shift of  $C_9$  by  $-0.5$  in M16 are possible. But what is interesting is that the decreased value of  $|V_{cb}|$  lowers also the SM result for the  $B_s \rightarrow \mu^+\mu^-$  rate so that with the NP shift central values from CMS and LHCb [15]

$$\overline{B}(B_s \rightarrow \mu^+\mu^-) = (2.8_{-0.6}^{+0.7}) \cdot 10^{-9}, \quad (24)$$

can be reached.

This value should be compared with central SM values

$$\overline{B}(B_s \rightarrow \mu^+\mu^-)_{\text{SM}} = 3.5 \cdot 10^{-9}, \quad \overline{B}(B_s \rightarrow \mu^+\mu^-)_{\text{SM}} = 3.2 \cdot 10^{-9} \quad (25)$$

for  $|V_{cb}| = 0.042$  and  $|V_{cb}| = 0.040$ , respectively. Thus within 331 models, on the whole, the results for  $\Delta F = 1$  for  $|V_{cb}| = 0.040$  appear more interesting than for  $|V_{cb}| = 0.042$ . As we will see below this is in particular the case for larger values of  $M_{Z'}$ .

Finally, we show in Fig. 8 the maximal value of  $\Delta(\varepsilon'/\varepsilon)$  for  $|V_{cb}| = 0.040$  as a function of  $|V_{ub}|$ . We observe that this value rises approximately linearly with increasing  $|V_{ub}|$  and for  $M_{Z'} = 3 \text{ TeV}$  and  $|V_{ub}| = 0.0044$  that is consistent with the inclusive determinations could reach values as high as  $\simeq 7.7 \times 10^{-4}$ . This possibility should be kept in mind even if such high values of  $|V_{ub}|$  seem rather unlikely as stated above. For  $|V_{cb}| = 0.042$  the effects of changing  $|V_{ub}|$  turn out to be smaller.

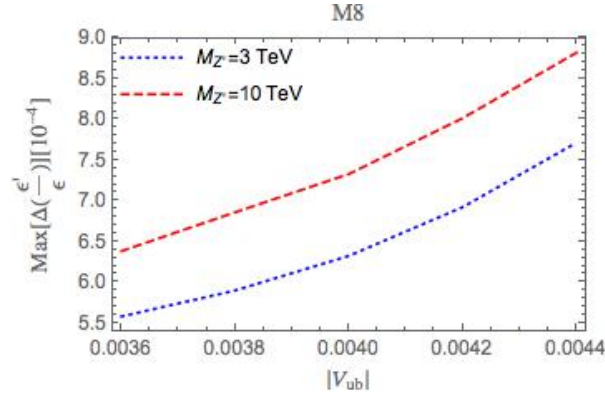


Figure 8: Maximal values of  $\Delta(\varepsilon'/\varepsilon)$  for  $|V_{cb}| = 0.040$  as function of  $|V_{ub}|$  for  $M_{Z'} = 3$  TeV and  $M_{Z'} = 10$  TeV.

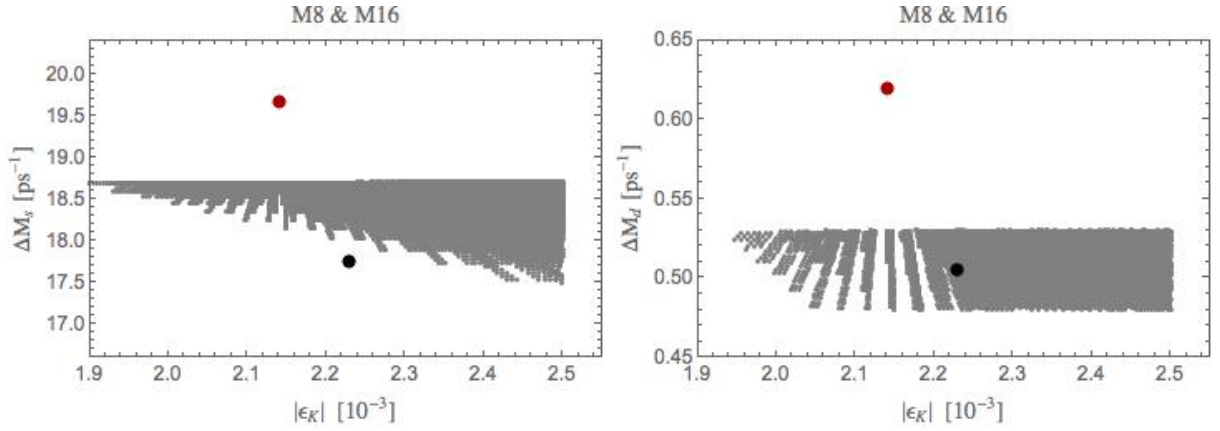


Figure 9:  $\Delta M_{s,d}$  vs.  $\varepsilon_K$  in M8 and M16. Red dots represent central SM values and black dots the central experimental values.  $M_{Z'} = 10$  TeV,  $|V_{cb}| = 0.042$  and  $|V_{ub}| = 0.0036$ .

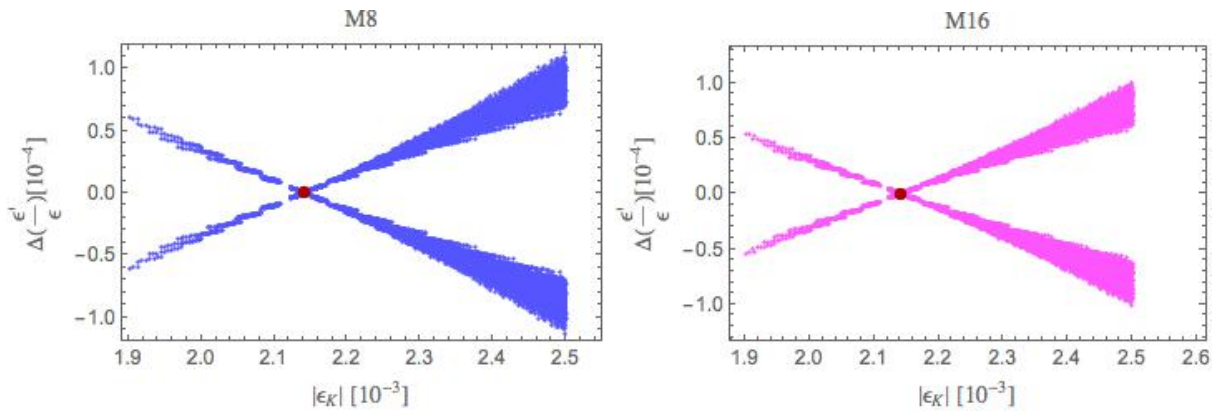


Figure 10:  $\Delta(\varepsilon'/\varepsilon)$  versus  $\varepsilon_K$  for M8 and M16. Red dot represents central SM values.  $M_{Z'} = 10$  TeV,  $|V_{cb}| = 0.042$  and  $|V_{ub}| = 0.0036$ .

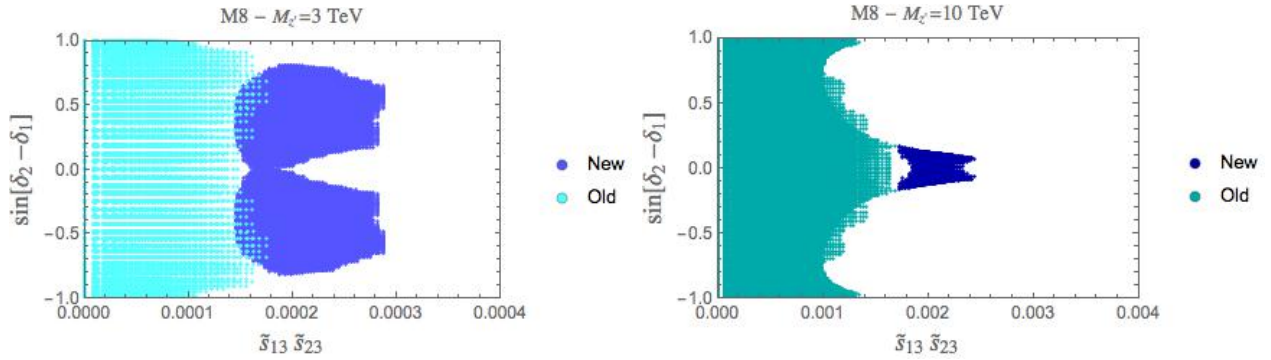


Figure 11: Allowed values of  $\sin(\delta_2 - \delta_1)$  and  $\tilde{s}_{13}\tilde{s}_{23}$  for M8 and  $M_{Z'} = 3$  TeV (left panel) and  $M_{Z'} = 10$  TeV (right panel). The old ranges are the ones from [23] and the new ones found here.  $|V_{cb}| = 0.042$  and  $|V_{ub}| = 0.0036$ .

Table 1: Summary of results for M8.  $|V_{ub}| = 0.0036$ .

$M_{Z'}$	$ V_{cb} $	$ \Delta(\varepsilon'/\varepsilon) _{max}(10^{-4})$	$\overline{B}(B_s \rightarrow \mu^+\mu^-)_{min}(10^{-9})$	$\text{Re}(C_9^{NP})_{min}$
3 TeV	0.042	6.2	3.21	-0.09
	0.040	5.9	2.69	-0.16
10 TeV	0.042	0.98	3.45	-0.02
	0.040	6.94	3.02	-0.05

## 2.4 $Z'$ Outside the Reach of the LHC

### 2.4.1 $|V_{ub}| = 0.042$

We will next investigate what happens when higher values of  $M_{Z'}$ , outside the reach of the LHC together with CKM parameters in (13), are considered. As an example we set  $M_{Z'} = 10$  TeV. In Fig. 9 we demonstrate that also in this case the tension between  $\Delta M_d$  and  $\varepsilon_K$  can be easily removed. In the case of  $\Delta M_s$  331 models perform much better than the SM represented by the red point so that the inclusion of the uncertainty in  $F_{B_s}\sqrt{\hat{B}_{B_s}}$  in (15), can bring easily 331 models to agree with data which is not possible within the SM. The question then arises what happens with NP effects in other observables for such high values  $M_{Z'}$ .

On the basis of our discussion in Section 4 in [23] we expect the effects in  $B_s \rightarrow \mu^+\mu^-$  and  $C_9$  to be smaller than for  $M_{Z'} = 3$  TeV, which can be confirmed as seen in Tables 1 and 2. On the other hand  $\varepsilon'/\varepsilon$  was found in [23] to be significantly enhanced for  $M_{Z'} = 10$  TeV as can be seen in Fig. 6 of that paper. Moreover through renormalization group effects it could be even enhanced slightly more than for  $M_{Z'} = 3$  TeV. However, as seen in Fig. 10, with new lattice constraints, this is no longer the case and the maximal allowed shifts in  $\varepsilon'/\varepsilon$  are below  $1 \times 10^{-4}$ , far too small to remove  $\varepsilon'/\varepsilon$  anomaly.

In order to understand this drastic change we recall the general formula for  $\varepsilon'/\varepsilon$  for arbitrary  $M_{Z'}$  in 331 models in the absence of  $Z - Z'$  mixing which is irrelevant in M8, M9 and M16 [23]

$$\left(\frac{\varepsilon'}{\varepsilon}\right)_{Z'} = \pm r_{\varepsilon'} 1.1 [\beta f(\beta)] \tilde{s}_{13}\tilde{s}_{23} \sin(\delta_2 - \delta_1) \left[\frac{B_8^{(3/2)}}{0.76}\right] \left[\frac{3 \text{ TeV}}{M_{Z'}}\right]^2 \quad (26)$$

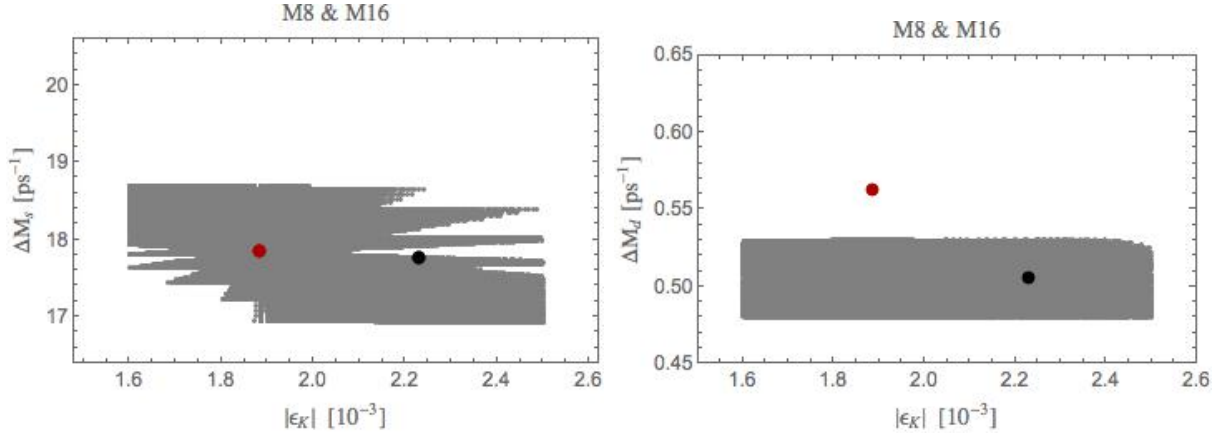


Figure 12:  $\Delta M_{s,d}$  vs.  $\varepsilon_K$  in M8 and M16. Red dots represent central SM values and black dots the central experimental values.  $M_{Z'}$  = 10 TeV,  $|V_{cb}|$  = 0.040 and  $|V_{ub}|$  = 0.0036.

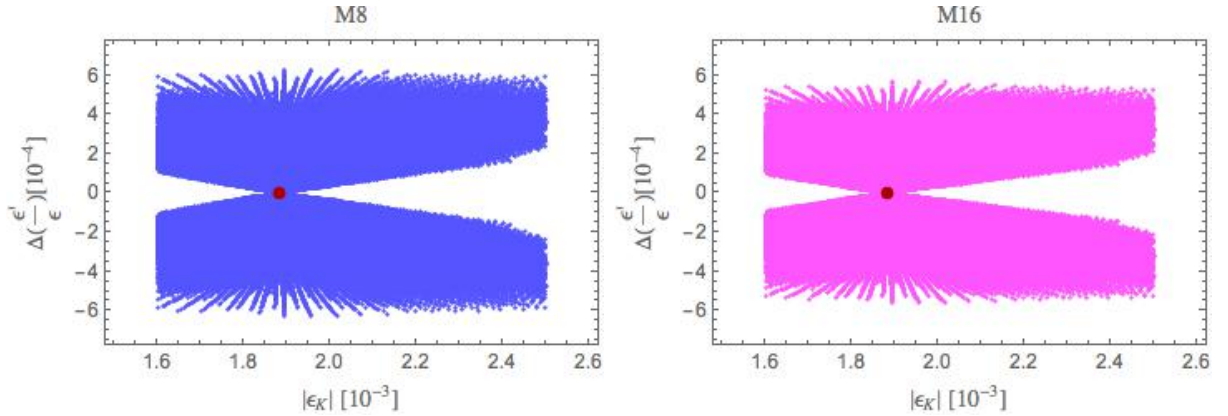


Figure 13:  $\Delta(\varepsilon'/\varepsilon)$  versus  $\varepsilon_K$  for M8. Red dot represents central SM values.  $M_{Z'}$  = 10 TeV,  $|V_{cb}|$  = 0.040 and  $|V_{ub}|$  = 0.0036.

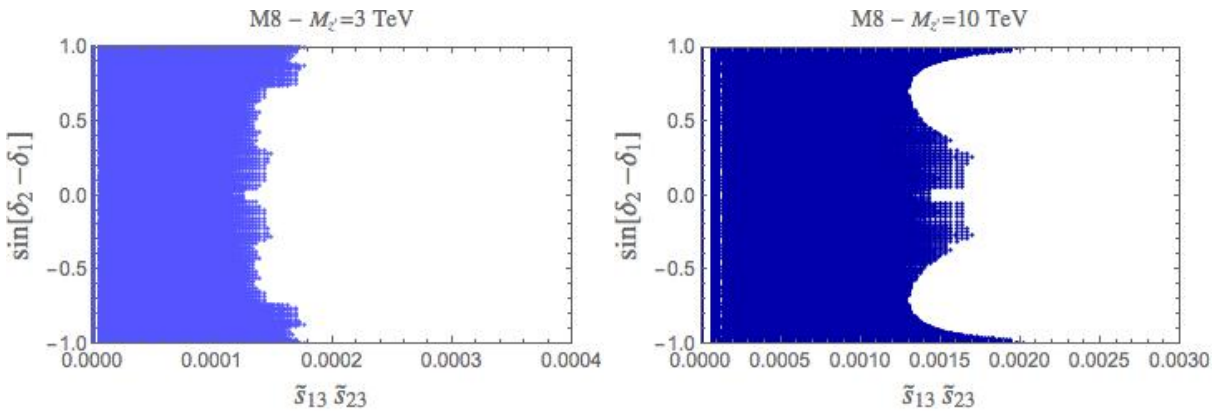


Figure 14: Allowed values of  $\sin(\delta_2 - \delta_1)$  and  $\tilde{s}_{13}\tilde{s}_{23}$  for M8 and  $M_{Z'} = 3$  TeV (left panel) and  $M_{Z'} = 10$  TeV (right panel).  $|V_{cb}|$  = 0.040 and  $|V_{ub}|$  = 0.0036.

Table 2: Summary of results for M16.  $|V_{ub}| = 0.0036$ .

$M_{Z'}$	$ V_{cb} $	$ \Delta(\varepsilon'/\varepsilon) _{max}(10^{-4})$	$\overline{B}(B_s \rightarrow \mu^+\mu^-)_{min}(10^{-9})$	$\text{Re}(C_9^{NP})_{min}$
3 TeV	0.042	5.55	3.40	-0.28
	0.040	5.17	3.01	-0.49
10 TeV	0.042	0.87	3.48	-0.05
	0.040	5.95	3.13	-0.15

with the upper sign for  $F_1$  and the lower for  $F_2$ .  $r_{\varepsilon'}$ ,  $\beta$  and  $f(\beta)$  are  $\mathcal{O}(1)$  so that only the remaining factors are of interest to us. Now as discussed in [23] with increasing  $M_{Z'}$  larger values of  $\tilde{s}_{13}$  and  $\tilde{s}_{23}$  are allowed by constraints from  $B_{s,d}^0 - \overline{B}_{s,d}^0$  mixing

$$\tilde{s}_{13}^{\max} \propto M_{Z'}, \quad \tilde{s}_{23}^{\max} \propto M_{Z'}, \quad (\Delta M_{s,d} \text{ constraints}). \quad (27)$$

In this manner the  $M_{Z'}$  suppression in (26) is compensated and the fate of  $\varepsilon'/\varepsilon$  depends on the allowed values of  $\sin(\delta_2 - \delta_1)$  that follow not only from  $\Delta M_{s,d}$  constraints but also from  $S_{\psi_{K_S}}$  and  $S_{\psi_\phi}$  constraints. Our analysis shows that whereas in our previous analysis values of  $\sin(\delta_2 - \delta_1) = 1$  were allowed this is no longer the case after new lattice results and maximal values of  $\sin(\delta_2 - \delta_1)$  are significantly below unity. While this suppression appears to be roughly compensated by the increase of the product  $\tilde{s}_{13}\tilde{s}_{23}^3$  for  $M_{Z'} = 3$  TeV, this is no longer the case for  $M_{Z'} = 10$  TeV and  $\varepsilon'/\varepsilon$  is strongly suppressed. This feature is clearly seen in Fig. 11, where the *old* ranges are the ones from [23] and the *new* ones found here.

#### 2.4.2 $|V_{cb}| = 0.040$

We next consider the CKM input in (23). The results for  $M_{Z'} = 10$  TeV are shown in Figs. 12–14. We observe:

- The tensions between  $\Delta M_{s,d}$  and  $\varepsilon_K$  can be much easier removed than for  $M_{Z'} = 3$  TeV because of the increased NP effects in  $\varepsilon_K$ . Comparing Fig. 12 with Fig. 8 we also observe that the agreement with data is better for  $|V_{cb}| = 0.040$ .
- The upward shift in  $\varepsilon'/\varepsilon$  up to  $(6-7) \times 10^{-4}$  is now possible so that  $\varepsilon'/\varepsilon$  with  $|V_{cb}| = 0.040$  can probe much higher mass scales than it is possible for  $|V_{cb}| = 0.042$  because of other constraints.
- The plots in Fig. 14 when compared with those in Fig. 11 explain why the NP effects in  $\varepsilon'/\varepsilon$  for  $|V_{cb}| = 0.040$  have a different structure than for  $|V_{cb}| = 0.042$ .  $\sin(\delta_2 - \delta_1)$  can for  $|V_{cb}| = 0.040$  reach unity even for  $M_{Z'} = 10$  TeV, while this is not possible for  $|V_{cb}| = 0.042$ .

As seen in Tables 1 and 2 NP effects in  $B_s \rightarrow \mu^+\mu^-$  and  $C_9$  are suppressed for  $M_{Z'} = 10$  TeV but not as much as for  $|V_{cb}| = 0.042$ .

All our results for M8 for different values of  $|V_{cb}|$  and  $M_{Z'}$  are summarized in Table 1. Very similar results are obtained for M9. The corresponding results for M16 are summarized

<sup>3</sup>These parameters must be larger in order to bring down the values of  $\Delta M_{s,d}$  to agree with data.



in Table 2. These tables show again how important is the precise determination of  $|V_{cb}|$  in tree-level decays.

Finally the red curve in Fig. 8 demonstrates that  $\Delta(\varepsilon'/\varepsilon)$  for  $|V_{cb}| = 0.040$  and  $M_{Z'} = 10$  TeV can for large values of  $|V_{ub}|$  reach values in the ballpark of  $\simeq 8.8 \times 10^{-4}$ . This increase relative to  $M_{Z'} = 3$  TeV is related to renormalization group effects as discussed in detail in [23].

## 3 The Simplest 331 Model: M0

### 3.1 Preliminaries

We will next look at the simplest 331 model recently proposed in [27] in which  $\beta = 0$ . We will denote it by M0. Even if this model fails to remove most of the anomalies in question, its simplicity invites us to have a closer look at its flavour structure. We will list  $Z'$  and  $Z$  couplings in this model and present formulae for  $C_9^{\text{NP}}$  and  $C_{10}^{\text{NP}}$  as well as  $\varepsilon'/\varepsilon$ . The expressions for  $\Delta F = 2$  processes and for  $B_s \rightarrow \mu^+ \mu^-$  as functions of the couplings listed below can be found in [20–22] and we will not repeat them here. One only has to set  $\beta = 0$  in that formulae. In this manner, in contrast to [27], we take  $Z - Z'$  mixing in all observables automatically into account.

### 3.2 $Z'$ Couplings

Setting  $\beta = 0$  in (17) of [21] we find for quark couplings

$$\Delta_L^{ij}(Z') = \frac{g_2}{\sqrt{3}} v_{3i}^* v_{3j}, \quad (28a)$$

$$\Delta_L^{ji}(Z') = [\Delta_L^{ij}(Z')]^*, \quad (28b)$$

$$\Delta_L^{d\bar{d}}(Z') = \Delta_L^{u\bar{u}}(Z') = \Delta_V^{d\bar{d}}(Z') = \Delta_V^{u\bar{u}}(Z') = -\frac{g_2}{2\sqrt{3}}, \quad (28c)$$

$$\Delta_A^{d\bar{d}}(Z') = \Delta_A^{u\bar{u}}(Z') = \frac{g_2}{2\sqrt{3}} \quad (28d)$$

$$\Delta_R^{d\bar{d}}(Z') = \Delta_R^{u\bar{u}}(Z') = 0. \quad (28e)$$

with  $v_{ij}$  given in (6).

The diagonal couplings given here are valid for the first two generations of quarks neglecting very small additional contributions [20]. For the third generation there is an additional term which can be found in (63) of [20]. It is irrelevant for our analysis of FCNCs but plays a role in electroweak precision tests [22]. For  $\beta = 0$  the diagonal  $b$  quark couplings differ from  $d$  and  $s$  couplings only by sign:

$$\Delta_L^{b\bar{b}}(Z') = \Delta_V^{b\bar{b}}(Z') = \frac{g_2}{2\sqrt{3}}, \quad \Delta_A^{b\bar{b}}(Z') = -\frac{g_2}{2\sqrt{3}}. \quad (29)$$

Setting  $\beta = 0$  in (18) of [21] we find for lepton couplings

$$\Delta_L^{\mu\bar{\mu}}(Z') = \Delta_L^{\nu\bar{\nu}}(Z') = \Delta_V^{\mu\bar{\mu}}(Z') = \frac{g_2}{2\sqrt{3}}, \quad (30a)$$

$$\Delta_A^{\mu\bar{\mu}}(Z') = \Delta_A^{\nu\bar{\nu}}(Z') = -\frac{g_2}{2\sqrt{3}}, \quad (30b)$$

$$\Delta_R^{\nu\bar{\nu}}(Z') = \Delta_R^{\mu\bar{\mu}}(Z') = 0 \quad (30c)$$

where we have defined

$$\begin{aligned} \Delta_V^{\mu\bar{\mu}}(Z') &= \Delta_R^{\mu\bar{\mu}}(Z') + \Delta_L^{\mu\bar{\mu}}(Z'), \\ \Delta_A^{\mu\bar{\mu}}(Z') &= \Delta_R^{\mu\bar{\mu}}(Z') - \Delta_L^{\mu\bar{\mu}}(Z'). \end{aligned} \quad (31)$$

These definitions also apply to other leptons and quarks. All these couplings are evaluated for  $\mu = M_{Z'}$  with  $g_2 = 0.633$  for  $M_{Z'} = 3 \text{ TeV}$ .

### 3.3 Z Couplings

The flavour non-diagonal couplings to quarks are generated from  $Z'$  couplings through  $Z - Z'$  mixing

$$\Delta_L^{ij}(Z) = \sin \xi \Delta_L^{ij}(Z'), \quad (32)$$

where using the general formula (10) in [22] we find for  $\beta = 0$

$$\sin \xi = a \frac{c_W}{\sqrt{3}} \left[ \frac{M_Z^2}{M_{Z'}^2} \right] = a 4.68 \times 10^{-4} \left[ \frac{3 \text{ TeV}}{M_{Z'}} \right]^2. \quad (33)$$

Here

$$-1 \leq a = \frac{1 - \tan^2 \bar{\beta}}{1 + \tan^2 \bar{\beta}} \leq 1, \quad \tan \bar{\beta} = \frac{v_\rho}{v_\eta} \quad (34)$$

with the scalar triplets  $\rho$  and  $\eta$  responsible for the masses of up-quarks and down-quarks, respectively. Thus for  $\tan \bar{\beta} = 1$  the parameter  $a = 0$  and the  $Z - Z'$  mixing vanish in agreement with [27]. On the other hand in the large  $\tan \bar{\beta}$  limit we find  $a = -1$  and in the low  $\tan \bar{\beta}$  limit one has  $a = 1$ .

The flavour diagonal  $Z$  couplings are the SM ones and collected in [21]. We evaluate them with  $g_2 = 0.652$  and  $\sin^2 \theta_W = 0.23116$  as valid at  $\mu = M_Z$ .

### 3.4 $C_9^{\text{NP}}$ and $C_{10}^{\text{NP}}$

The corrections from NP to the Wilson coefficients  $C_9$  and  $C_{10}$  that weight the semileptonic operators in the effective hamiltonian relevant for  $b \rightarrow s\mu^+\mu^-$  transitions are given as follows

$$\sin^2 \theta_W C_9^{\text{NP}} = -\frac{1}{g_{\text{SM}}^2 M_{Z'}^2} \frac{\Delta_L^{sb}(Z') \Delta_V^{\mu\bar{\mu}}(Z')}{V_{ts}^* V_{tb}} (1 + R_{\mu\mu}^V), \quad (35)$$

$$\sin^2 \theta_W C_{10}^{\text{NP}} = -\frac{1}{g_{\text{SM}}^2 M_{Z'}^2} \frac{\Delta_L^{sb}(Z') \Delta_A^{\mu\bar{\mu}}(Z')}{V_{ts}^* V_{tb}} (1 + R_{\mu\mu}^A). \quad (36)$$

As seen in these equations  $C_9^{\text{NP}}$  involves leptonic vector coupling of  $Z'$  while  $C_{10}^{\text{NP}}$  the axial-vector one.  $C_9^{\text{NP}}$  is crucial for  $B_d \rightarrow K^* \mu^+ \mu^-$ ,  $C_{10}^{\text{NP}}$  for  $B_s \rightarrow \mu^+ \mu^-$  and both coefficients are relevant for  $B_d \rightarrow K \mu^+ \mu^-$ .

Here

$$g_{\text{SM}}^2 = 4 \frac{M_W^2 G_F^2}{2\pi^2} = 1.78137 \times 10^{-7} \text{ GeV}^{-2}, \quad (37)$$

with  $G_F$  being the Fermi constant. The terms  $R_{\mu\mu}^V$  and  $R_{\mu\mu}^A$  are generated by  $Z - Z'$  mixing and are given as follows

$$R_{\mu\mu}^V = \sin \xi \left[ \frac{M_{Z'}^2}{M_Z^2} \right] \left[ \frac{\Delta_V^{\mu\mu}(Z)}{\Delta_V^{\mu\mu}(Z')} \right], \quad (38)$$

$$R_{\mu\mu}^A = \sin \xi \left[ \frac{M_{Z'}^2}{M_Z^2} \right] \left[ \frac{\Delta_A^{\mu\mu}(Z)}{\Delta_A^{\mu\mu}(Z')} \right], \quad (39)$$

For  $\beta = 0$  we find then

$$\sin^2 \theta_W C_9^{\text{NP}} = -\frac{1}{g_{\text{SM}}^2 M_{Z'}^2} \frac{g_2^2(M_{Z'})}{6} \left[ \frac{v_{32}^* v_{33}}{V_{ts}^* V_{tb}} \right] (1 + R_{\mu\mu}^V), \quad (40)$$

$$\sin^2 \theta_W C_{10}^{\text{NP}} = +\frac{1}{g_{\text{SM}}^2 M_{Z'}^2} \frac{g_2^2(M_{Z'})}{6} \left[ \frac{v_{32}^* v_{33}}{V_{ts}^* V_{tb}} \right] (1 + R_{\mu\mu}^A) \quad (41)$$

with

$$R_{\mu\mu}^V = -0.08 a, \quad R_{\mu\mu}^A = -1.02 a \quad (42)$$

that do not depend on  $M_{Z'}$  except for logarithmic  $M_{Z'}$  dependence of  $g_2$ . The numerical factors above correspond to  $M_{Z'} = 3 \text{ TeV}$ .

We observe then that in the absence of  $Z - Z'$  mixing ( $a = 0$ ), independently of the parameters  $v_{ij}$ , the following phenomenologically successful relation

$$C_9^{\text{NP}} = -C_{10}^{\text{NP}}, \quad (a = 0) \quad (43)$$

holds. This should be contrasted with models M8, M9 and M16 for which we found [23]

$$C_9^{\text{NP}} = 0.49 C_{10}^{\text{NP}} \quad (\text{M8}), \quad C_9^{\text{NP}} = 0.42 C_{10}^{\text{NP}} \quad (\text{M9}). \quad (44)$$

The result in (43) differs also from

$$C_9^{\text{NP}} = -4.59 C_{10}^{\text{NP}} \quad (\text{M16}) \quad (45)$$

which is close to one of the favourite solutions in which NP resides dominantly in the coefficient  $C_9$ . Thus already on the basis of  $B$  physics observables we should be able to distinguish between the models M0, (M8,M9) and M16.

However in the presence of  $Z - Z'$  mixing the relation (43) does not hold. While this effect is small in  $C_9^{\text{NP}}$ , it can be large in  $C_{10}^{\text{NP}}$ , in particular for  $a = 1$ , when  $C_{10}^{\text{NP}}$  becomes very small and the suppression of the rate for  $B_s \rightarrow \mu^+ \mu^-$  is absent. More interesting is then the case of  $a \approx -1$ , corresponding to large  $\tan \bar{\beta}$ , as then the simultaneous suppressions of  $C_9$  through  $C_9^{\text{NP}}$  and of  $B_s \rightarrow \mu^+ \mu^-$  rate through  $C_{10}^{\text{NP}}$  are stronger. We find then

$$C_9^{\text{NP}} \approx -0.5 C_{10}^{\text{NP}}, \quad (a \approx -1), \quad (46)$$

that on a qualitative level is still a better description of the data than the results in (44) and (45). But the crucial question is whether the values of both coefficients are sufficiently large when all constraints are taken into account. Before answering this question let us make a closer look at  $\varepsilon'/\varepsilon$  in this model.

### 3.5 $\varepsilon'/\varepsilon$

#### 3.5.1 Preliminaries

The analyses of  $\varepsilon'/\varepsilon$  in 331 models with  $\beta \neq 0$  have been presented by us in [22,23]. We want to generalize them to the case  $\beta = 0$ . Generally in 331 models we have

$$\left(\frac{\varepsilon'}{\varepsilon}\right)_{331} = \left(\frac{\varepsilon'}{\varepsilon}\right)_{\text{SM}} + \left(\frac{\varepsilon'}{\varepsilon}\right)_Z + \left(\frac{\varepsilon'}{\varepsilon}\right)_{Z'} \equiv \left(\frac{\varepsilon'}{\varepsilon}\right)_{\text{SM}} + \Delta(\varepsilon'/\varepsilon) \quad (47)$$

with the  $\Delta(\varepsilon'/\varepsilon)$  resulting from tree-level  $Z'$  and  $Z$  exchanges.

Now, as demonstrated by us in [22], the shift  $\Delta(\varepsilon'/\varepsilon)$  is governed in 331 models by the electroweak  $(V - A) \times (V + A)$  penguin operator

$$Q_8 = \frac{3}{2} (\bar{s}_\alpha d_\beta)_{V-A} \sum_{q=u,d,s,c,b,t} e_q (\bar{q}_\beta q_\alpha)_{V+A} \quad (48)$$

with only small contributions from other operators. This result applies to both  $Z$  and  $Z'$  contributions with the latter ones significantly more important as demonstrated in [22]. Here we would like to point out that this pattern is not valid for  $\beta = 0$ .

Indeed as seen in (41) of [22] the important coefficient  $C_7(M_{Z'})$  generated by tree-level  $Z'$  exchange for  $\beta \neq 0$  vanishes for  $\beta = 0$  and consequently,  $Q_8$  operator cannot be generated from  $Q_7$  operator by renormalization group effects. Contributions of other operators are very small so that  $Z'$  contributions to  $\varepsilon'/\varepsilon$  can be neglected. This is directly related to the fact, as seen in (28e), that the diagonal right-handed couplings of  $Z'$  to quarks vanish for  $\beta = 0$ . But for  $Z$  such couplings are present implying that tree-level  $Z$  exchanges can provide a shift in  $\varepsilon'/\varepsilon$ .

#### 3.5.2 $Z$ Contribution

The inclusion of this contribution is straightforward as the only thing to be done is to calculate the shifts from NP in the functions  $X$ ,  $Y$  and  $Z$  that enter the SM model contribution to  $\varepsilon'/\varepsilon$ . One finds then [22]

$$\Delta X = \Delta Y = \Delta Z = \sin \xi c_W \frac{8\pi^2 \text{Im} \Delta_L^{sd}(Z')}{g_2^3 \text{Im} \lambda_t} \quad (49)$$

where  $g_2 = 0.652$  and  $\lambda_t = V_{td} V_{ts}^*$ . Replacing then the SM functions  $X_0(x_t)$ ,  $Y_0(x_t)$  and  $Z_0(x_t)$  by

$$X = X_0(x_t) + \Delta X, \quad Y = Y_0(x_t) + \Delta Y, \quad Z = Z_0(x_t) + \Delta Z \quad (50)$$

in the phenomenological formula formula (90) for  $\varepsilon'/\varepsilon$  in [8] allows to take automatically the first two contributions in (47) in 331 models into account.

Inserting  $\sin \xi$  in (33) and the  $Z'$  coupling into (49) we obtain for  $\beta = 0$

$$\Delta X = \Delta Y = \Delta Z = 47.6 a \left[ \frac{M_Z^2}{M_{Z'}^2} \right] \frac{\text{Im}(v_{32}^* v_{31})}{\text{Im} \lambda_t}. \quad (51)$$

Evidently for  $a = 0$ , as done in [27], NP contributions to  $\varepsilon'/\varepsilon$  from  $Z$  exchanges vanish and as the ones from  $Z'$  can be neglected,  $\varepsilon'/\varepsilon$  is full governed by the SM contribution. This appears

presently problematic in view of the findings in [7–9, 38] that a significant upwards shift  $\varepsilon'/\varepsilon$  of at least  $5 \times 10^{-4}$  is required to bring the theory to agree with the data from NA48 [10] and KTeV [11, 12] collaborations.

The question then arises whether including  $Z - Z'$  mixing we can obtain the required positive shift in  $\varepsilon'/\varepsilon$ . But, as seen in (46), in order to preserve at least partly the pattern in (43) we are interested in

$$-1 \leq a < 0, \quad \tan \bar{\beta} > 1. \quad (52)$$

In order to answer this question we insert (51) into (90) in Appendix B of [8] to obtain first

$$\Delta(\varepsilon'/\varepsilon) = \Delta(\varepsilon'/\varepsilon)_Z = 47.6 a \left[ \frac{M_Z^2}{M_{Z'}^2} \right] [P_X + P_Y + P_Z] \text{Im}(v_{32}^* v_{31}). \quad (53)$$

From Table 5 in [8] we find then for the central value of  $\alpha_s(M_Z)$ :

$$P_X + P_Y + P_Z = 1.52 + 0.12 R_6 - 13.65 R_8 \quad (54)$$

where

$$R_6 \equiv B_6^{(1/2)} \left[ \frac{114.54 \text{ MeV}}{m_s(m_c) + m_d(m_c)} \right]^2, \quad R_8 \equiv B_8^{(3/2)} \left[ \frac{114.54 \text{ MeV}}{m_s(m_c) + m_d(m_c)} \right]^2. \quad (55)$$

Now the results from the RBC-UKQCD collaboration imply the following values for  $B_6^{(1/2)}$  and  $B_8^{(3/2)}$  [8, 39]

$$B_6^{(1/2)} = 0.57 \pm 0.19, \quad B_8^{(3/2)} = 0.76 \pm 0.05, \quad (\text{RBC-UKQCD}) \quad (56)$$

that are compatible with the bounds from large  $N$  approach [9]

$$B_6^{(1/2)} \leq B_8^{(3/2)} < 1 \quad (\text{large-}N). \quad (57)$$

Using then the results in (56) we find

$$P_X + P_Y + P_Z = -8.78 \pm 0.68 \quad (58)$$

and finally

$$\Delta(\varepsilon'/\varepsilon) = -a (0.39 \pm 0.03) \left[ \frac{3 \text{ TeV}}{M_{Z'}} \right]^2 \text{Im}(v_{32}^* v_{31}). \quad (59)$$

The question then arises whether for  $a$  in the range (52) one can get sufficient shift in  $\varepsilon'/\varepsilon$  while satisfying other constraints. In particular the ones from  $\Delta F = 2$  transitions, where as seen in the previous section the SM experiences tensions in its predictions for  $\Delta M_{s,d}$  and  $\varepsilon_K$ .

In Fig. 15 we show  $\Delta M_{s,d}$  vs.  $\varepsilon_K$  in M0. Red dots represent central SM values and black dots the central experimental values. We observe that the tensions between  $\Delta M_{s,d}$  vs.  $\varepsilon_K$  present in the SM can be removed in the M0 model. But as seen in Fig. 16 the shift in  $\varepsilon'/\varepsilon$  can be at most  $1.1 \times 10^{-4}$  which is far too small to be able to remove  $\varepsilon'/\varepsilon$  anomaly. Moreover, this maximal shift can only be obtained for the maximal  $Z - Z'$  mixing. We have checked using the expressions in [22] that then the fit to EWPO is significantly worse than the one

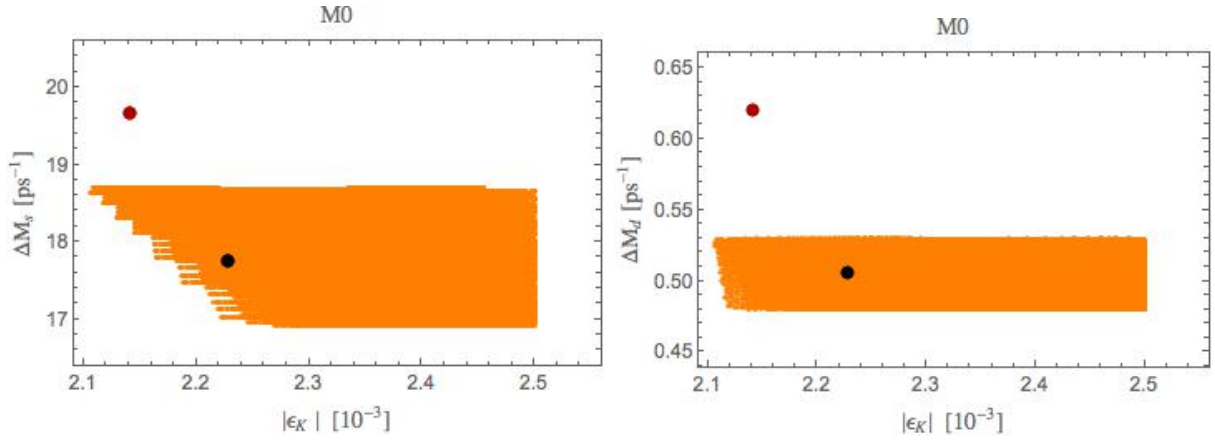


Figure 15:  $\Delta M_{s,d}$  vs.  $\varepsilon_K$  in  $M0$ . Red dots represent central SM values and black dots the central experimental values.  $M_{Z'}$  = 3 TeV and  $|V_{cb}|$  = 0.042.

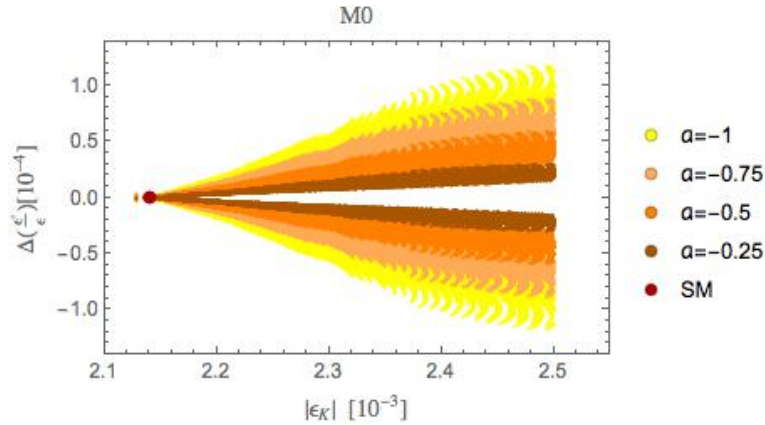


Figure 16:  $\Delta(\varepsilon'/\varepsilon)$  versus  $\varepsilon_K$  for  $M0$  for several values of the  $Z - Z'$  mixing parameter  $a$ .  $M_{Z'}$  = 3 TeV and  $|V_{cb}|$  = 0.042.

in the SM, whereas the three models analysed in the previous section perform better in these tests than the SM [22].

We do not show the results for  $C_9$  and  $B_s \rightarrow \mu^+\mu^-$  as NP effects are significantly smaller than in M8 and M16. Thus even if M0 can remove the tensions between  $\Delta M_{s,d}$  and  $\varepsilon_K$ , it fails badly in the case of other anomalies and therefore cannot compete with models M8, M9 and M16, unless all anomalies disappear one day.

## 4 Summary

Motivated by the recently improved results from the Fermilab Lattice and MILC Collaborations on the hadronic matrix elements entering  $\Delta M_{s,d}$  in  $B_{s,d}^0 - \bar{B}_{s,d}^0$  mixing [5] and the resulting increased tensions between  $\Delta M_{s,d}$  and  $\varepsilon_K$  in the SM and generally CMFV models [4], we have performed a new analysis of 331 models. In order to illustrate the sensitivity of the results to the modification of hadronic parameters we have first used the CKM input of our previous

analysis in [23] that is given in (13). In addition, in order to illustrate the sensitivity of the results to the value of  $|V_{cb}|$  we have also performed the analysis with the CKM input in (23), where  $|V_{cb}|$  is lower than in (13). We also investigated  $|V_{ub}|$  dependence.

The most important results of our analysis, summarized in Tables 1 and 2 are as follows:

- The tensions between  $\Delta M_{s,d}$  and  $\varepsilon_K$  can be removed in the three 331 models with  $\beta \neq 0$  (M8, M9, M16) considered by us and this for both CKM inputs. This turns out to be also possible in the model with  $\beta = 0$  (M0) in the case of the input (13) but it is much harder when  $|V_{cb}|$  is smaller as in (23).
- Models M8, M9 and M16 can provide a positive shift in  $\varepsilon'/\varepsilon$  up to  $6 \times 10^{-4}$  for  $M_{Z'} = 3 \text{ TeV}$  for both choices of  $|V_{cb}|$  and  $|V_{ub}| = 0.0036$ . But in contrast to our previous analysis this shift decreases fast with increasing  $M_{Z'}$  in the case of  $|V_{cb}| = 0.042$  but its maximal values are practically unchanged for  $M_{Z'} = 10 \text{ TeV}$  when  $|V_{cb}| = 0.040$  is used. We also find that for  $|V_{cb}| = 0.040$  and the inclusive values of  $|V_{ub}|$  the maximal shifts in  $\varepsilon'/\varepsilon$  are increased to  $7.7 \times 10^{-4}$  and  $8.8 \times 10^{-4}$  for  $M_{Z'} = 3 \text{ TeV}$  and  $M_{Z'} = 10 \text{ TeV}$ , respectively. In the model M0, in which NP contribution to  $\varepsilon'/\varepsilon$  is governed by  $Z - Z'$  mixing, NP effects are very small even for  $M_{Z'} = 3 \text{ TeV}$ .
- In M8 and M9 the rate for  $B_s \rightarrow \mu^+ \mu^-$  can be reduced by at most 10% and 20% for  $M_{Z'} = 3 \text{ TeV}$  and  $|V_{cb}| = 0.042$  and  $|V_{cb}| = 0.040$ , respectively. This can bring the theory within  $1 \sigma$  range of the combined result from CMS and LHCb and for  $|V_{cb}| = 0.040$  one can even reach the present central experimental value of this rate (24). The maximal shifts in  $C_9$  are  $C_9^{\text{NP}} = -0.1$  and  $C_9^{\text{NP}} = -0.2$  for these two  $|V_{cb}|$  values, respectively. This is only a moderate shift and these models do not really help in the case of  $B_d \rightarrow K^* \mu^+ \mu^-$  anomalies.
- In M16 the situation is opposite. The rate for  $B_s \rightarrow \mu^+ \mu^-$  can be reduced for  $M_{Z'} = 3 \text{ TeV}$  for the two  $|V_{cb}|$  values by at most 3% and 10%, respectively but with the corresponding values  $C_9^{\text{NP}} = -0.3$  and  $-0.5$  the anomaly in  $B_d \rightarrow K^* \mu^+ \mu^-$  can be partially reduced.
- In M0 NP effects in  $\varepsilon'/\varepsilon$ ,  $B_s \rightarrow \mu^+ \mu^-$  and  $B_d \rightarrow K^* \mu^+ \mu^-$  are too small to be relevant. Therefore our analysis demonstrates that in the presence of the anomalies discussed by us the  $U(1)_X$  factor in the gauge group of 331 models cannot be  $U(1)_Y$ .
- For higher values of  $M_{Z'}$  the effects in  $B_s \rightarrow \mu^+ \mu^-$  and  $B_d \rightarrow K^* \mu^+ \mu^-$  are much smaller. We recall that NP effects in rare  $K$  decays and  $B \rightarrow K(K^*) \nu \bar{\nu}$  remain small in all 331 models even for  $M_{Z'}$  of few TeV.

Even if models M8, M9, M16 still compete with each other and M0 does not appear to be phenomenologically viable from present perspective, our feeling is that eventually only models M8 and M9 have a chance to survive future tests if the anomalies discussed by us will be confirmed in the future. The point is that with present theoretical uncertainties in  $B_d \rightarrow K^* \mu^+ \mu^-$  NP effects, even in M16, will be hardly seen in this decay. The decay  $B_s \rightarrow \mu^+ \mu^-$  is much cleaner and in the flavour precision era 15 – 20% effects from NP, which are only possible in M8 and M9, could in principle be distinguished from SM predictions but this would require very large reduction in the experimental error on its rate.

Thus the main virtue of 331 models as opposed to SM and CMFV models is the ability to remove the tensions between  $\Delta M_{s,d}$  and  $\varepsilon_K$  and simultaneously provide a significant upward shift in  $\varepsilon'/\varepsilon$  but only for lower values of  $|V_{cb}|$  can this property remain for  $M_{Z'}$  beyond the LHC reach. The possibility of a significant suppression of the rate for  $B_s \rightarrow \mu^+ \mu^-$  in M8 and M9 for  $|V_{cb}| = 0.040$  is also a welcome feature. In particular, as it is correlated with the maximal shift in  $\varepsilon'/\varepsilon$ .

While the NP pattern in flavour physics identified by us in 331 models is interesting, we should hope that eventually NP contributions to flavour observables are larger than found in these models and are also significant in rare  $K$  decays which are theoretically very clean and in  $B \rightarrow K(K^*)\nu\bar{\nu}$  which are cleaner than  $B \rightarrow K(K^*)\mu^+\mu^-$  decays. Most importantly the comparison of our results in [23], prior to the lattice results in [5], with the ones obtained using this new input demonstrates clearly how the shifts and increased accuracy in non-perturbative parameters can have important impact on the size of NP effects. Similar comment can be made in connection with  $|V_{cb}|$ .

## Acknowledgements

This research was done and financed in the context of the ERC Advanced Grant project “FLAVOUR” (267104) and has also been carried out within the INFN project (Iniziativa Specifica) QFT-HEP. It was partially supported by the DFG cluster of excellence “Origin and Structure of the Universe”.

## References

- [1] A. J. Buras and J. Girrbach, *Towards the Identification of New Physics through Quark Flavour Violating Processes*, *Rept. Prog. Phys.* **77** (2014) 086201, [arXiv:1306.3775].
- [2] F. Pisano and V. Pleitez, *An  $SU(3) \times U(1)$  model for electroweak interactions*, *Phys. Rev.* **D46** (1992) 410–417, [hep-ph/9206242].
- [3] P. H. Frampton, *Chiral dilepton model and the flavor question*, *Phys. Rev. Lett.* **69** (1992) 2889–2891.
- [4] M. Blanke and A. J. Buras, *Universal Unitarity Triangle 2016 and the tension between  $\Delta M_{s,d}$  and  $\varepsilon_K$  in CMFV models*, *Eur. Phys. J.* **C76** (2016), no. 4 197, [arXiv:1602.04020].
- [5] A. Bazavov et al.,  *$B_{(s)}^0$ -mixing matrix elements from lattice QCD for the Standard Model and beyond*, arXiv:1602.03560.
- [6] T. Blum et al.,  *$K \rightarrow \pi\pi$   $\Delta I = 3/2$  decay amplitude in the continuum limit*, *Phys. Rev.* **D91** (2015), no. 7 074502, [arXiv:1502.00263].
- [7] **RBC, UKQCD** Collaboration, Z. Bai et al., *Standard Model Prediction for Direct CP Violation in  $K$  Decay*, *Phys. Rev. Lett.* **115** (2015), no. 21 212001, [arXiv:1505.07863].



- 
- [8] A. J. Buras, M. Gorbahn, S. Jäger, and M. Jamin, *Improved anatomy of  $\varepsilon'/\varepsilon$  in the Standard Model*, *JHEP* **11** (2015) 202, [[arXiv:1507.06345](#)].
- [9] A. J. Buras and J.-M. Gerard, *Upper Bounds on  $\varepsilon'/\varepsilon$  Parameters  $B_6^{(1/2)}$  and  $B_8^{(3/2)}$  from Large  $N$  QCD and other News*, *JHEP* **12** (2015) 008, [[arXiv:1507.06326](#)].
- [10] **NA48** Collaboration, J. Batley et al., *A Precision measurement of direct CP violation in the decay of neutral kaons into two pions*, *Phys. Lett.* **B544** (2002) 97–112, [[hep-ex/0208009](#)].
- [11] **KTeV** Collaboration, A. Alavi-Harati et al., *Measurements of direct CP violation, CPT symmetry, and other parameters in the neutral kaon system*, *Phys. Rev.* **D67** (2003) 012005, [[hep-ex/0208007](#)].
- [12] **KTeV** Collaboration, E. Abouzaid et al., *Precise Measurements of Direct CP Violation, CPT Symmetry, and Other Parameters in the Neutral Kaon System*, *Phys. Rev.* **D83** (2011) 092001, [[arXiv:1011.0127](#)].
- [13] A. J. Buras and J.-M. Gerard, *Final State Interactions in  $K \rightarrow \pi\pi$  Decays:  $\Delta I = 1/2$  Rule vs.  $\varepsilon'/\varepsilon$* , [arXiv:1603.05686](#).
- [14] A. J. Buras, D. Buttazzo, and R. Knegjens,  *$K \rightarrow \pi\nu\bar{\nu}$  and  $\varepsilon'/\varepsilon$  in Simplified New Physics Models*, *JHEP* **11** (2015) 166, [[arXiv:1507.08672](#)].
- [15] **LHCb, CMS** Collaboration, V. Khachatryan et al., *Observation of the rare  $B_s^0 \rightarrow \mu^+\mu^-$  decay from the combined analysis of CMS and LHCb data*, *Nature* **522** (2015) 68–72, [[arXiv:1411.4413](#)].
- [16] C. Bobeth, M. Gorbahn, T. Hermann, M. Misiak, E. Stamou, et al.,  *$B_{s,d} \rightarrow \ell^+\ell^-$  in the Standard Model with Reduced Theoretical Uncertainty*, *Phys. Rev. Lett.* **112** (2014) 101801, [[arXiv:1311.0903](#)].
- [17] **ATLAS** Collaboration, M. Aaboud et al., *Study of the rare decays of  $B_s^0$  and  $B^0$  into muon pairs from data collected during the LHC Run 1 with the ATLAS detector*, [arXiv:1604.04263](#).
- [18] W. Altmannshofer and D. M. Straub, *New physics in  $b \rightarrow s$  transitions after LHC run 1*, *Eur. Phys. J.* **C75** (2015), no. 8 382, [[arXiv:1411.3161](#)].
- [19] S. Descotes-Genon, L. Hofer, J. Matias, and J. Virto, *Global analysis of  $b \rightarrow s\ell\ell$  anomalies*, [arXiv:1510.04239](#).
- [20] A. J. Buras, F. De Fazio, J. Girrbach, and M. V. Carlucci, *The Anatomy of Quark Flavour Observables in 331 Models in the Flavour Precision Era*, *JHEP* **1302** (2013) 023, [[arXiv:1211.1237](#)].
- [21] A. J. Buras, F. De Fazio, and J. Girrbach, *331 models facing new  $b \rightarrow s\mu^+\mu^-$  data*, *JHEP* **1402** (2014) 112, [[arXiv:1311.6729](#)].

- [22] A. J. Buras, F. De Fazio, and J. Girrbach-Noe, *Z-Z' mixing and Z-mediated FCNCs in  $SU(3)_C \times SU(3)_L \times U(1)_X$  Models*, *JHEP* **1408** (2014) 039, [arXiv:1405.3850].
- [23] A. J. Buras and F. De Fazio,  *$\varepsilon'/\varepsilon$  in 331 Models*, *JHEP* **03** (2016) 010, [arXiv:1512.02869].
- [24] R. A. Diaz, R. Martinez, and F. Ochoa,  *$SU(3)(c) \times SU(3)(L) \times U(1)(X)$  models for beta arbitrary and families with mirror fermions*, *Phys. Rev.* **D72** (2005) 035018, [hep-ph/0411263].
- [25] A. Carcamo Hernandez, R. Martinez, and F. Ochoa, *Z and Z' decays with and without FCNC in 331 models*, *Phys. Rev.* **D73** (2006) 035007, [hep-ph/0510421].
- [26] C. Promberger, S. Schatt, and F. Schwab, *Flavor Changing Neutral Current Effects and CP Violation in the Minimal 3-3-1 Model*, *Phys. Rev.* **D75** (2007) 115007, [hep-ph/0702169].
- [27] L. T. Hue and L. D. Ninh, *The simplest 3-3-1 model*, arXiv:1510.00302.
- [28] C. DeTar, *LQCD: Flavor Physics and Spectroscopy*, arXiv:1511.06884.
- [29] **MILC** Collaboration, J. A. Bailey et al., *BD form factors at nonzero recoil and  $|V_{cb}|$  from 2+1-flavor lattice QCD*, *Phys. Rev.* **D92** (2015), no. 3 034506, [arXiv:1503.07237].
- [30] **Fermilab Lattice, MILC** Collaboration, J. A. Bailey et al.,  *$|V_{ub}|$  from  $B \rightarrow \pi \ell \nu$  decays and (2+1)-flavor lattice QCD*, *Phys. Rev.* **D92** (2015), no. 1 014024, [arXiv:1503.07839].
- [31] **Belle** Collaboration, R. Glattauer et al., *Measurement of the decay  $B \rightarrow D \ell \nu_\ell$  in fully reconstructed events and determination of the Cabibbo-Kobayashi-Maskawa matrix element  $|V_{cb}|$* , arXiv:1510.03657.
- [32] **LHCb** Collaboration, R. Aaij et al., *Determination of the quark coupling strength  $|V_{ub}|$  using baryonic decays*, *Nature Phys.* **11** (2015) 743–747, [arXiv:1504.01568].
- [33] A. Alberti, P. Gambino, K. J. Healey, and S. Nandi, *Precision Determination of the Cabibbo-Kobayashi-Maskawa Element  $V_{cb}$* , *Phys. Rev. Lett.* **114** (2015) 061802, [arXiv:1411.6560].
- [34] P. Gambino, K. J. Healey, and C. Mondino, *NNVub: a Neural Network Approach to  $B \rightarrow X_u \ell \nu$* , arXiv:1604.07598.
- [35] **CKMfitter Group** Collaboration, K. Trabelsi, *World average and experimental overview of  $\gamma/\varphi_3$ ; presented at CKM 2014*, . <http://www.ckmfitter.in2p3.fr>.
- [36] **ETM** Collaboration, N. Carrasco et al., *B-physics from  $N_f = 2$  tmQCD: the Standard Model and beyond*, *JHEP* **1403** (2014) 016, [arXiv:1308.1851].

- 
- [37] **Heavy Flavor Averaging Group (HFAG)** Collaboration, Y. Amhis et al., *Averages of  $b$ -hadron,  $c$ -hadron, and  $\tau$ -lepton properties as of summer 2014*, arXiv:1412.7515. <http://www.slac.stanford.edu/xorg/hfag>.
- [38] A. J. Buras, *New physics patterns in  $\varepsilon'/\varepsilon$  and  $\varepsilon_K$  with implications for rare kaon decays and  $\Delta M_K$* , *JHEP* **04** (2016) 071, [arXiv:1601.00005].
- [39] A. J. Buras, D. Buttazzo, J. Girrbach-Noe, and R. Knegjens,  *$K^+ \rightarrow \pi^+ \nu \bar{\nu}$  and  $K_L \rightarrow \pi^0 \nu \bar{\nu}$  in the Standard Model: status and perspectives*, *JHEP* **11** (2015) 033, [arXiv:1503.02693].